

SIMULATION AND MODELLING OF MEMS CANTILEVER BEAM FOR LOW PULL-IN VOLTAGES

A DISSERTATION

SUBMITTED IN PARTIAL FULFILLMENT OF THE REQUIREMENTS
FOR THE AWARD OF THE DEGREE
OF

MASTER OF TECHNOLOGY
IN
COMPUTER AIDED ANALYSIS AND DESIGN

Submitted by:

RITWIK MEHROTRA

(2023/CAD/06)

Under the supervision of

Dr. SANJAY KUMAR



**DEPARTMENT OF MECHANICAL ENGINEERING
DELHI TECHNOLOGICAL UNIVERSITY**

(Formerly Delhi College of Engineering)
Bawana Road, Delhi-110042

MAY, 2025

DEPARTMENT OF MECHANICAL ENGINEERING
DELHI TECHNOLOGICAL UNIVERSITY
(Formerly Delhi College of Engineering)
Bawana Road, Delhi-110042

CANDIDATE DECLARATION

I, RITWIK MEHROTRA, Roll No. 2023/CAD/06 student of M.Tech Computer Aided Analysis and Design, hereby declare that the project Dissertation titled “Simulation and Modelling of MEMS Cantilever Beam for Low Pull-in Voltages” which is submitted by me to the Department of Mechanical Engineering, Delhi Technological University, Delhi in partial fulfilment of the requirement for the award of the degree of Master of Technology, is original and not copied from any source without proper citation. This work has not previously formed the basis for the award of any Degree, Diploma Associateship, Fellowship or other similar title or recognition.

Place: Delhi

Date:

RITWIK MEHROTRA

DEPARTMENT OF MECHANICAL ENGINEERING
DELHI TECHNOLOGICAL UNIVERSITY
(Formerly Delhi College of Engineering)
Bawana Road, Delhi-110042

CERTIFICATE

I hereby certify that the Project Dissertation titled “Simulation and Modelling of MEMS Cantilever Beam for Low Pull-in Voltages” which is submitted by **Ritwik Mehrotra**, Roll No. **2023/CAD/06**, Department of Mechanical Engineering, Delhi Technological University, Delhi in partial fulfilment of the requirement for the award of the degree of Master of Technology, is a record of the project work carried out by the student under my supervision. To the best of knowledge this work has not been submitted in part or full for any Degree or Diploma to this University or elsewhere.

Place: Delhi

Date:

Dr. SANJAY KUMAR
ASSOCIATE PROFESSOR
SUPERVISOR

ABSTRACT

This thesis presents in-depth simulation and modelling study on electrostatically driven MEMS cantilever beam switches with a main goal of obtaining low pull-in voltage for efficient and dependable operation in low-power electronic systems. MEMS switches are increasingly important in modern technology because of their possible miniaturization, high speed switching, low power consumption, and integration into complex microsystems. This work aims to meet this challenge by investigating, using COMSOL Multiphysics 6.2, several structural and material parameters on the performance of a cantilever-based MEMS switch through finite element simulation.

Ten independent configurations in all were modelled, varying key parameters including the cantilever beam material (gold and polysilicon), the electrode material (aluminium, copper, and gold), the beam dimensions (small and large), and the presence or absence of a dielectric layer between the beam and the electrode. Each configuration was painstakingly modelled with physics-driven meshing (set to a fine level), and the simulations included electromechanical coupling to faithfully record the interaction between the electrostatic force generated by the applied voltage and the resulting mechanical deformation of the cantilever beam. The main focus of the study was extensive performance measurements covering pull-in voltage, maximum displacement, and von Mises stress distribution across the structure.

The results revealed clearly different performance depending on configurations. Particularly, a design combining a gold cantilever beam of larger dimensions with an aluminium electrode without dielectric layer showed the lowest pull-in voltage yet maintaining structural integrity. Rising as the most likely candidate for practical use, it struck a good mix between mechanical flexibility and electrostatic efficiency. To match normal voltage levels from 1.V to 10.V, the original voltage sweep—from 0.V to 9.15'V in fine steps was scaled and interpolated, so improving the interpretability and usability of the simulation results. This conversion enabled simpler integration into system-level circuit simulations or control strategies, helped to better analyse data, and present information.

Especially for applications requiring ultra-low power consumption and exceptional sensitivity, the results of this work provide perceptive study of MEMS switch design and optimisation. This thesis develops a strong simulation framework by methodically evaluating the effects of geometric and material changes, so guiding both future research and practical development in the field of MEMS. Moreover, the method applied in this work combining parametric modelling, high-resolution simulation, and data scaling may provide a basis for extending this work into real-world testing of MEMS cantilever switches.

ACKNOWLEDGEMENT

I would like to express my sincere gratitude to my guide, **Dr. SANJAY KUMAR**, as Associate Professor in the Department of Mechanical Engineering, for his invaluable guidance, support and expertise throughout the course of this research project. His constant encouragement, insightful feedback, and dedication have been instrumental in shaping the direction and progress of this work. His extensive knowledge and passionate commitment to the subject matter inspired me to pursue excellence and challenge myself to investigate new dimensions of MEMS (Micro Electro Mechanical Systems) cantilever switch modelling and the design of devices utilizing electrostatic actuation.

I would also like to extend my heartfelt appreciation to **Prof. B.B. ARORA**, Head of the Department of Mechanical Engineering, for his support and encouragement. His vision and leadership have provided a conducive environment for academic and research pursuits. I am grateful for his valuable insights and guidance that have contributed to the overall success of this project.

Lastly, I would like to acknowledge my family and friends for their unwavering support, encouragement, and understanding throughout this research endeavour. Their love, belief in my abilities, and motivation have been the driving force behind my perseverance and determination.

RITWIK MEHROTRA

2023/CAD/06

M.Tech (CAAD)

Delhi Technological University

TABLE OF CONTENTS

CANDIDATE DECLARATION.....	ii
CERTIFICATE.....	iii
ABSTRACT.....	iv
ACKNOWLEDGEMENT	vi
TABLE OF CONTENTS.....	vii
LIST OF TABLES.....	xi
LIST OF FIGURES	xii
NOMENCLATURE	xiv
CHAPTER 1 INTRODUCTION	1
1.1 Overview of MEMS.....	1
1.2 Cantilever Beams in MEMS	2
1.3 Pull-in Phenomenn.....	3
1.4 Problem Statement	5
1.5 Research Gaps and Thesis Contribution	5
1.6 Motivation for Low Pull-in Voltage and Cantilever Beam.....	6
1.7 Objectives.....	7
1.8 Scope of Thesis	8
1.9 Related Works.....	9
1.9.1 Biomedical Implants and Microvalves.....	9
1.9.2 Aerospace and Defense Systems	10
1.9.3 Wearable Sensors and IoT Devices.....	10
1.9.4 Environmental and Structural Monitoring.....	11
CHAPTER 2 LITERATURE REVIEW	12
2.1 Analytical Modelling	12
2.2 Numerical Simulation Method.....	13

2.2.1 Full Field Analysis and Mechanical Response.....	13
2.2.2 Geometric and Material Parameters Sweeping	13
2.3 The Critical Role of Dielectric Interface.....	14
2.4 Strategies to Lower Pull-in Voltage.....	15
2.4.1 Geometric Optimization	15
2.5 Advanced Modelling and Performance Optimizarion	16
CHAPTER 3 METHODOLOGY	18
3.1 Introduction.....	18
3.2 Software and Physics Interface	18
3.3 Geometric Modelling	19
3.3.1 Configuration A (Larger beam and electrode)	19
3.3.2 Configuration B (Larger beam and electrode).....	20
3.4 Materials Properties	21
3.5 Boundary Conditions and Electrical Loading	22
3.5.1 Solid Mechanics	22
3.5.2 Electrostatics.....	22
3.5.3 Multiphysics Integration.....	23
3.6 Mesh Configuration	24
3.6.1 Meshing Type and Control Settings	24
3.6.2 Refinements.....	24
3.7 Analytical Pull-in Voltage Estimation	25
3.7.1 Pull-in Voltage without Dielectric Layer	25
3.7.2 Pull-in Voltage with Dielectric Layer	26
3.7.3 The 1/3 Rule and Pull-in Instability	26
3.8 Study and Solver Settings	26
3.9 Simulation Cases and Evaluation Metrics.....	27
CHAPTER 4 RESULTS AND DISCUSSION.....	29

4.1 Introduction	29
4.2 Beam Displacement vs Voltage Behaviour.....	29
4.2.1 Case C1 (Gold, Bigger Beam, Al Electrode, with Layer	30
4.2.2 Case C2 (Gold, Smaller Beam, Al Electrode, with Layer.....	31
4.2.3 Case C3 (Gold, Bigger Beam, Cu Electrode, with Layer.....	32
4.2.4 Case C4 (Gold, Smaller Beam, Cu Electrode, with Layer	34
4.2.5 Case C5 (Gold, Smaller Beam, Cu Electrode, no Layer	35
4.2.6 Case C6 (Polysilicon, Bigger Beam, Al Electrode, with Layer	36
4.2.7 Case C7 (Polysilicon, Smaller Beam, Al Electrode, with Layer.....	37
4.2.8 Case C8 (Polysilicon, Smaller Beam, Al Electrode, no Layer.....	39
4.2.9 Case C9 (Polysilicon, Bigger Beam, Gold Electrode, with Layer	40
4.2.10 Case C10 (Polysilicon, Smaller Beam, Al Electrode, with Layer.....	42
4.3 Overview of Simulation Cases.....	44
4.4 Discussion	45
4.4.1 Effect of Beam Material	45
4.4.2 Effect of Beam Geometry.....	46
4.4.3 The Impact of the Electrode Material.....	47
4.4.3.1 Aluminium (Al)	47
4.4.3.2 Copper (Cu)	47
4.4.3.1 Gold (Au)	48
4.4.4 The Dielectric Layer's Effect (Silicon Nitride).....	48
4.4.4.1 The primary effect of introducing a dielectric layer is.....	49
4.4.4.2 Without a dielectric layer in Cases 5,8 and 10	49
4.5 Analytical Validation of Simulated Pull-In Voltage.....	50
4.6 von Mises Stress Analysis.....	51
4.6.1 Case C1 (Gold, Bigger Beam, Al Electrode, with Layer	52
4.6.2 Case C2 (Gold, Smaller Beam, Al Electrode, with Layer.....	53

4.6.3 Case C3 (Gold, Bigger Beam, Cu Electrode, with Layer.....	54
4.6.4 Case C4 (Gold, Smaller Beam, Cu Electrode, with Layer	55
4.6.5 Case C5 (Gold, Smaller Beam, Cu Electrode, no Layer	56
4.6.6 Case C6 (Polysilicon, Bigger Beam, Al Electrode, with Layer	57
4.6.7 Case C7 (Polysilicon, Smaller Beam, Al Electrode, with Layer.....	58
4.6.8 Case C8 (Polysilicon, Smaller Beam, Al Electrode, no Layer.....	59
4.6.9 Case C9 (Polysilicon, Bigger Beam, Gold Electrode, with Layer	60
4.6.10 Case C10 (Polysilicon, Smaller Beam, Al Electrode, with Layer.....	61
4.7 Summary of Key Findings and Design Implications	63
CHAPTER 5 CONCLUSION AND FUTURE WORK.....	64
5.1 Conclusion.....	64
5.1.1 Pull-in Voltage Behaviour.....	64
5.1.2 von Mises Stress Analysis	65
5.1.3 Electrodes Area and Beam Geometry	66
5.1.4 Including the Dielectric Layer.....	66
5.2 Future Work	67
REFERENCES	68

LIST OF TABLES

TABLE 3.1 SUMMARY OF MATERIAL PROPERTIES.....	21
TABLE 3.2 OVERVIEW OF SIMULTAION CASES.....	28
TABLE 4.1 DISPLACEMENT FIELD VS VOLTAGE TABLE OF C1	30
TABLE 4.2 DISPLACEMENT FIELD VS VOLTAGE TABLE OF C2	31
TABLE 4.3 DISPLACEMENT FIELD VS VOLTAGE TABLE OF C3	33
TABLE 4.4 DISPLACEMENT FIELD VS VOLTAGE TABLE OF C4	35
TABLE 4.5 DISPLACEMENT FIELD VS VOLTAGE TABLE OF C5	36
TABLE 4.6 DISPLACEMENT FIELD VS VOLTAGE TABLE OF C6	37
TABLE 4.7 DISPLACEMENT FIELD VS VOLTAGE TABLE OF C7.....	38
TABLE 4.8 DISPLACEMENT FIELD VS VOLTAGE TABLE OF C8	40
TABLE 4.9 DISPLACEMENT FIELD VS VOLTAGE TABLE OF C9	41
TABLE 4.10 DISPLACEMENT FIELD VS VOLTAGE TABLE OF C10	43
TABLE 4.11 COMPARISON OF PULL-IN VOLTAGES AND MAXIMAUM DISPLACEMENT FOR DIFFERENT MEMS SWITCH CONFIGURATION	44
TABLE 4.12 EFFECT OF BEAM MATERIAL	46
TABLE 4.13 EFFECT OF BEAM GEOMETRY	47
TABLE 4.14 SUMMARY OF ELECTRODE MATERIAL INFLUENCE	48
TABLE 4.15 SUMMARY OF DIELECTRIC LAYER INFLUENCE.....	49
TABLE 4.16 COMPARISON B/W ANALYTICAL AND SIMULATED PULL-IN VOLTAGES.....	50
TABLE 4.17 KEY FINDINGS SYNOPSIS AND DESIGN IMPLICATION	63

LIST OF FIGURES

FIGURE 3.1 SELECTION OF PHYSICS	19
FIGURE 3.2 CONFIGURATION OF LARGER BEAM AND ELECTRODE RESPECTIVELY	19
FIGURE 3.3 GEOMETRY OF CONFIGURATION A	20
FIGURE 3.4 CONFIGURATION OF SMALLER BEAM AND ELECTRODE RESPECTIVELY	20
FIGURE 3.5 GEOMETRY OF CONFIGURATION B	21
FIGURE 3.6 FIXED CONSTRAINTS	22
FIGURE 3.7 APPLIED VOLTAGE ON ELECTRODE	23
FIGURE 3.8 GROUNDED BEAM	23
FIGURE 3.9 MESHING	24
FIGURE 3.10 SHOWING SOLVER PARAMETERS AND CONVERGENCE SETTINGS	27
FIGURE 4.1 BENDING OF BEAM	29
FIGURE 4.2 BEAM DISPLACEMENT BEHAVIOUR OF C1	30
FIGURE 4.3 BEAM DISPLACEMENT VS VOLTAGE GRAPH OF C1	30
FIGURE 4.4 BEAM DISPLACEMENT BEHAVIOUR OF C2	31
FIGURE 4.5 BEAM DISPLACEMENT VS VOLTAGE GRAPH OF C2	31
FIGURE 4.6 BEAM DISPLACEMENT BEHAVIOUR OF C3	32
FIGURE 4.7 BEAM DISPLACEMENT VS VOLTAGE GRAPH OF C3	33
FIGURE 4.8 BEAM DISPLACEMENT BEHAVIOUR OF C4	34
FIGURE 4.9 BEAM DISPLACEMENT VS VOLTAGE GRAPH OF C4	34
FIGURE 4.10 BEAM DISPLACEMENT BEHAVIOUR OF C5	35
FIGURE 4.11 BEAM DISPLACEMENT VS VOLTAGE GRAPH OF C5	35
FIGURE 4.12 BEAM DISPLACEMENT BEHAVIOUR OF C6	36
FIGURE 4.13 BEAM DISPLACEMENT VS VOLTAGE GRAPH OF C6	37
FIGURE 4.14 BEAM DISPLACEMENT BEHAVIOUR OF C7	37
FIGURE 4.15 BEAM DISPLACEMENT VS VOLTAGE GRAPH OF C7	38
FIGURE 4.16 BEAM DISPLACEMENT BEHAVIOUR OF C8	39
FIGURE 4.17 BEAM DISPLACEMENT VS VOLTAGE GRAPH OF C8	39
FIGURE 4.18 BEAM DISPLACEMENT BEHAVIOUR OF C9	40
FIGURE 4.19 BEAM DISPLACEMENT VS VOLTAGE GRAPH OF C9	41
FIGURE 4.20 BEAM DISPLACEMENT BEHAVIOUR OF C10	42
FIGURE 4.21 BEAM DISPLACEMENT VS VOLTAGE GRAPH OF C10	43
FIGURE 4.22 PULL-IN VOLTAGE GRAPH	44

FIGURE 4.23 MAXIMUM DISPLACEMENT GRAPH	45
FIGURE 4.24 ANALYTICAL VS SIMULATED PULL-IN VOLTAGE.....	51
FIGURE 4.25 STRESS DISTRIBUTION WITHIN THE CNTILEVER BEAM FOR CASE C1	52
FIGURE 4.26 VON MISES STRESS VS VOLTAGE GRAPH OF C1	52
FIGURE 4.27 STRESS DISTRIBUTION WITHIN THE CNTILEVER BEAM FOR CASE C2	53
FIGURE 4.28 VON MISES STRESS VS VOLTAGE GRAPH OF C2	53
FIGURE 4.29 STRESS DISTRIBUTION WITHIN THE CNTILEVER BEAM FOR CASE C3	54
FIGURE 4.30 VON MISES STRESS VS VOLTAGE GRAPH OF C3	54
FIGURE 4.31 STRESS DISTRIBUTION WITHIN THE CNTILEVER BEAM FOR CASE C4	55
FIGURE 4.32 VON MISES STRESS VS VOLTAGE GRAPH OF C4	55
FIGURE 4.33 STRESS DISTRIBUTION WITHIN THE CNTILEVER BEAM FOR CASE C5	56
FIGURE 4.34 VON MISES STRESS VS VOLTAGE GRAPH OF C5	56
FIGURE 4.35 STRESS DISTRIBUTION WITHIN THE CNTILEVER BEAM FOR CASE C6	57
FIGURE 4.36 VON MISES STRESS VS VOLTAGE GRAPH OF C6	57
FIGURE 4.37 STRESS DISTRIBUTION WITHIN THE CNTILEVER BEAM FOR CASE C7	58
FIGURE 4.38 VON MISES STRESS VS VOLTAGE GRAPH OF C7	58
FIGURE 4.39 STRESS DISTRIBUTION WITHIN THE CNTILEVER BEAM FOR CASE C8	59
FIGURE 4.40 VON MISES STRESS VS VOLTAGE GRAPH OF C8	59
FIGURE 4.41 STRESS DISTRIBUTION WITHIN THE CNTILEVER BEAM FOR CASE C9	60
FIGURE 4.42 VON MISES STRESS VS VOLTAGE GRAPH OF C9	60
FIGURE 4.43 STRESS DISTRIBUTION WITHIN THE CNTILEVER BEAM FOR CASE C10	61
FIGURE 4.44 VON MISES STRESS VS VOLTAGE GRAPH OF C10	61
FIGURE 4.45 MAXIMUM VON MISES STRESS GRAPH.....	62

NOMENCLATURE

b	Width of cantilever beam (μm)
COMSOL	COMSOL Multiphysics simulation software
E	Young's modulus (GPa)
ϵ_0	Permittivity of free space ($8.854 \times 10^{-12} \text{ F/m}$)
ϵ_r	Relative permittivity of dielectric material
FEM	Finite Element Method
g_0	Initial gap between beam and electrode (μm)
h	Thickness of cantilever beam (μm)
I	Area moment of Inertia (μm^4)
K_{eq}	Equivalent Spring constant of the cantilever beam (N/m)
L	Length of cantilever beam (μm)
MEMS	Micro-Electro-Mechanical Systems
ρ	Density (kg/m^3)
σ	Von Mises stress (MPa)
t_d	Thickness of dielectric layer (μm)
u	Displacement (μm)
V_0	Applied voltage (V)
V_{Pi}	Pull-in voltage (V)
ν	Poisson's ratio

CHAPTER 1

INTRODUCTION

1.1 Overview of MEMS

Microelectromechanical systems (MEMS) are a new technology that integrate mechanical and electrical properties into a single chip, usually silicon. MEMS systems tend to be considered small systems, which are dimensioned in micrometres or millimetres, and have benefits of size reduction, performance, power consumption, manufacturing costs, and integration with microelectronic components. [1] MEMS are interdisciplinary; they utilize knowledge from electrical engineering, mechanical engineering, materials sciences, and physics to develop even smaller but often more functional devices. The concept of reduced machines was first proposed by Richard Feynman, in his famous 1959 lecture It's Plenty of Room at the Bottom, in which he speculated about the ability to manipulate atoms and molecules on a basis of one at a time. Although the original concepts about MEMS technologies were primarily theoretical, the discovery of techniques for fabricating integrated circuits (ICs) in the 1960s and 1970s sparked the conception of real instances of MEMS. For example, the resonant gate transistor by Nathanson and others in 1967 and silicon pressure sensors from the 1970s. More students and researchers began utilizing bulk micromachining and surface micromachining in the 1980s and 1990s to form more complex 3D structures; leading to a flourishing MEMS community.[3]

MEMS devices can be classified broadly based on their function:

- **Sensors:** Convert a physical stimulus (e.g., pressure, acceleration, temperature, chemical concentration, light, etc.) into an electrical signal. Smartphone accelerometers, automotive pressure sensors, or micro-cantilever-based biosensors are some examples.
- **Actuators:** Convert an electrical signal into mechanical motion or force. Some common examples are micro-mirrors used for optical switching, micro-pumps for fluidic control, and micro-switches for RF applications.
- **Transducers:** These devices convert energies from one form to another. This vague wording encompasses both sensors and actuators.

These developments allow for precise manipulation of feature size and material properties at the micro-scale. It is widely recognized that silicon is the most common microstructure material due to its advantageous mechanical properties (high Young's modulus, low hysteresis), established material processing, and compatibility with CMOS integration. Nevertheless, for special applications there are also other materials, such as polymers, metals, and ceramics, that offer methods of micro-manufacturing. MEMS technologies also have an impact that is found everywhere, with many new innovations appearing on the market each year. Examples of MEMS consumer electronic items include MEMS accelerometers and gyroscopes, which provide motion detection in smartphones, game consoles, and wearable electronics (wristwatches). Examples of MEMS applications in the automotive sector include MEMS sensors for safety features (air bag activation), MEMS sensors for engine control, and MEMS sensors for tire and other pressure sensors. Examples in the biomedical sector can include drug delivery, lab on a chip diagnostic device, and implantable sensors. Since MEMS devices are small, inexpensive, and well managed and since they provide high performance, they have emerged as critical components of new "technological systems".

1.2 Cantilever Beams in MEMS

The cantilever beam is one of the simplest and most prevalent types of MEMS structure. A cantilever beam is defined as a beam that is supported at one end and free to deform at one end. Its simple and predictable mechanical behaviour makes it a perfect building block for MEMS devices. Due to their flexibility and scalability, cantilever beams can be incorporated in many possible micro-scale systems, leading them to utilize either as passive components or active transducers.[2]

Cantilever beams are often used as the moving part that deflects towards an underlying electrode upon the application of a control voltage in the framework of MEMS switches. The deflection arises from electrostatic attraction between the electrode and the beam. The beam quickly collapses onto the electrode if the voltage rises above a threshold referred to as the pull-in voltage. At micro sizes, RF and digital circuits use this abrupt change in displacement to generate an ON/OFF switching action.[5]

A cantilever beam in MEMS exhibits mechanical behaviour influenced by several parameters including its material properties (e.g., Young's modulus, density), geometric dimensions (length, width, thickness), and boundary conditions. The pull-in voltage, displacement range, stress distribution, and switching performance are much influenced

by extra design factors including the gap between the beam and the electrode, dielectric layer inclusion, and type of the electrode material.

Cantilever beams can be used for sensing components in order to detect external force, mass change, or environmental changes.

An example of this includes:

- **Atomic Force Microscope (AFM) probes:** The deflection of a sharp tip on a cantilever can be used to generate nanoscale surface topographies for high-resolution imaging.
- **Chemical and Biosensors:** Cantilever surfaces can be functionalized to selectively absorb specific molecules or biological agents. A mass change or surface stress on a cantilever surface will cause the cantilever to deflect or change its fundamental resonant frequency and will allow the detection of pathogens, toxins or chemical compound at very small concentrations [13].
- **Temperature Sensors:** Bimetallic cantilevers have two or more materials bonded together to form a single specific geometry, so when the temperature changes, the differences in thermal expansion will either bend the cantilever shape down or up. The amount of temperature change can be mapped using the resultant bend in the cantilever beam as a measurement.
- **Force Sensors:** Bending of cantilevers can be directly related to a force applied, so cantilevers can be used for small micro-force measurement.

1.3 Pull-in Phenomenon

A critical phenomenon related to electrostatically actuated MEMS devices, specifically cantilever beams, is a "pull-in" instability. When a voltage is applied between the movable electrode (i.e., a cantilever beam, etc.) and a fixed electrode, an attractive electrostatic force is created. As a function of the applied voltage, the electrostatic force increases, causing the movable electrode to move towards the fixed electrode. Eventually, the applied voltage reaches a critical value, called a "pull-in voltage" at which the electrostatic force exceeds the restoring mechanical force (provided by the elasticity of the beam), at this stage there is an unstable equilibrium. At this point, the movable electrode snaps to contact the fixed electrode, irrespective of any increase in the applied voltage. This irreversible collapse of an electrostatically actuated cantilever beam limits the useable operating range of electrostatic MEMS devices, and also can lead to device

failure if not properly mitigated [3]. To properly design and operate electrostatic MEMS, it is important to understand the pull-in phenomena and take it into account.

The phenomenon of pull-in occurs because the electrostatic force has a non-linear relationship with the displacement of the gap. As the cantilever beam is deflected, the gap between the beam and the fixed electrode decreases. This results in a positive feedback loop: additional deflection will increase the electrostatic force, which will increase the deflection. This feedback loop will continue until reaching a critical point where the mechanical restoring force of the beam cannot balance the exponentially growth of the electrostatic force. For this basic parallel-plate model, the critical point occurs when the movable electrode has travelled approximately one-third the original gap distance. After this "one-third rule" has been deflected, any further increase in the applied voltage or simply maintaining the pull-in voltage will instantly cause the beam to be mechanically unstable and snap down. This instability phenomenon is similar to mechanical buckling. For a simplified parallel-plate representation, we define the critical engagement point as the position of the movable electrode when it has moved approximately one-third of the original gap. After the "one-third rule" deflection position is reached, increased voltage applied to the beam, or at pulling voltage allows the beam to experience mechanical instability and snap down. This is akin to mechanical buckling instability.

The impact of pull-in can have large implications for MEMS device performance:

- **Operational Limit:** Pull-in voltage defines the maximum usable voltage for an electrostatically actuated device because above this value the device will experience instability.
- **Hysteresis:** Once the device has pulled in, it will typically take a voltage (release voltage) that is less than the pull-in voltage to return to its original position which generates hysteresis in the voltage-deflection curve.
- **Stiction Risk:** The snap-down behaviour during the pull-in can cause the movable electrode to adhere permanently (stiction) to the fixed electrode, particularly if humidity levels are high or surface forces dominate, which renders the device permanently inoperable [21].
- **Damage:** The force of the snap down can damage structural or dielectric layers which decreases the device lifetime.

Thus, it is crucial in the design of electrostatically actuated MEMS that the pull-in voltage is predicted and controlled accurately.

1.4 Problem Statement

Predicting and managing the pull-in voltage, which sets the switch's operating voltage, is one such challenge. This voltage depends on factors like the beam's shape, material properties electrode dimensions, and the air gap. Standard analytical models provide basic estimations but often overlook nonlinear effects caused by complex 3D deformations, fringe electric fields, and dielectric layers.

Another big issue is the mechanical stress in the cantilever beam while it works. Shrinking device sizes and higher voltages can lead to stress building up near fixed supports. This stress might result in wear or even failure over time. To predict how long a device will last, we must understand how stress spreads and how it relates to the materials used and the size of the beams.

Device lifetime depends on a complete knowledge of stress distribution and its connection with beam size and materials. Comprehensive simulation studies that simultaneously consider geometric fluctuations, dielectric effects, and coupled electromechanical behaviour are still much needed despite much of study. Such investigations should also verify accuracy and practical relevance by means of validation of simulation results against analytical models.

This work intends to investigate the electromechanical performance of MEMS cantilever switches under variations in beam and electrode materials (e.g., gold, polysilicon, aluminium), beam dimensions, and dielectric layer inclusion. The aim is to suggest the best configuration depending on important criteria including von Mises stress, maximum displacement and pull-in voltage.

1.5 Research Gaps and Thesis Contribution

Although MEMS switch modelling using FEM tools like COMSOL has made great progress, many significant problems and research gaps still exist, especially with relation to the thorough knowledge and mitigating of dielectric interface effects in particular material systems. Even if individual elements like pull-in voltage, contact mechanics, and dielectric charging have been investigated in isolation or with simplified assumptions, a truly complete COMSOL-based model that methodically investigates the coupled electromechanical behaviour of gold beam-type switches with silicon nitride dielectric interfaces is still needed. Sometimes existing literature simplifies the complex dynamics of charge accumulation, the exact influence of different dielectric thickness on both static and dynamic performance, and the long-term effect on release characteristics

for this specific material combination. Many studies either ignore entirely the transitory effects of dielectric charge on both actuation and release, focus on other dielectric materials, or use simpler contact models.

This thesis tries to close these specific gaps by means of a comprehensive and complete COMSOL Multiphysics 6.2 model. This model will faithfully reflect the complex electromechanical coupling, reasonable contact dynamics, and specific effects of silicon nitride dielectric layers including possible transient charging events on the performance and long-term dependability of gold beam-type MEMS switches. This work will methodically investigate the exact influence of dielectric layer thickness on pull-in voltage, contact force, and release voltage. By means of a deeper, more integrated knowledge of the design trade-offs inherent in this material system, this work will offer insightful analysis so optimizing future MEMS switch topologies for improved performance, dependability, and extended operational lifetime.

1.6 Motivation for Low Pull-in Voltage and Cantilever Beam

There are multiple reasons for the motivation to achieve low pull-in voltages in MEMS cantilever beams, and individual reason comprise factors that may reduce utility and performance in general terms, in the entire application context:

- **CMOS Compatibility:** Most microelectronic control circuits that utilize CMOS can only operate at very low voltages (3V, 5V, 10V). A design for MEMS cantilever beams that requires low pull-in voltage allows for electrical integration with conventional standard CMOS without general consideration. This means that there is no need for separate, complex, bulky high-voltage external drivers or charge pumps. Lower pull-in voltage leads to a much simpler overall system design and lower system cost, and allow true system-on-chip (SoC) implementations, i.e. MEMS and electronics on the same substrate [11].
- **Increased Reliability and Lifetime:** Operating an electrical device, such as a MEMS cantilever, at lower voltages will always decrease the chances of device failure due to dielectric breakdown, electromigration, and other voltage induced mechanisms of degradation. For electrostatic actuators operating in air, as the electric fields across the air gap increase, there are increasing chances of charge trapping, material degradation, and degradation leading to dielectric failure. As a pull-in voltage gets decreased, the electric fields created are decreased and so will

help to improve the lifetime and reliability of the cantilever device long term [12]. It is important for medical implants or any industrial sensor where it will be in use for the long-term.

- **Increased Sensitivity (for sensors):** In many sensor applications using cantilevers, a pull-in can itself be a means of detection, or certainly, the device can operate and remain consistently near a pull-in to maximize a response. A lower pull-in voltage means that the cantilever exhibits the appropriate mechanical compliance or is demonstrating that the electrostatic force can overcome the mechanical restoring force with a smaller amount of applied potential. Thus, this directly relates to being able to have increased sensitivity to any small outside forces (e.g. small changes in pressure, mass, or chemical concentration) that may create a small dynamic deflection that will push the cantilever towards the pull-in point. This also means that there will be a smaller disturbance in the environment to trigger the pull-in event, which means better speed and responsiveness of the sensor. [11]

1.7 Objectives

- To investigate the mechanical reaction of a MEMS cantilever beam under electrostatic actuation and, in particular, stress history, deflection response, and nonlinear instability and pull-in.
- To create and validate simulation workflows using COMSOL Multiphysics to model and investigate the electromechanical behaviour of the cantilever beam and its pull-in voltage.
- To conduct parametric work using COMSOL Multiphysics to study the effects of key geometrical parameters (length, width, thickness, initial gap) on the pull-in voltage. Two beam sizes ($250\text{ }\mu\text{m} \times 130\text{ }\mu\text{m} \times 1.5\text{ }\mu\text{m}$) and ($140\text{ }\mu\text{m} \times 75\text{ }\mu\text{m} \times 1.5\text{ }\mu\text{m}$) will be investigated to see how mechanical stresses and operational voltage are affected by miniaturising.
- To model the electromechanical coupling behaviour of the beam using COMSOL Multiphysics, harnessing physics-based models (Solid Mechanics and Electrostatics) to produce results for comparison with analytical approximations.

- To compare and contrast the pull-in voltage of various material (gold, aluminium, copper, polysilicon) configurations and dimensions and find the best mechanically operative design for the lowest actuation voltage before failure.
- Comparing examples with and without silicon nitride dielectric layers helps one to quantify the effect of dielectric layers on device performance. This includes investigating variations in effective air gap, electric field strengths, pull-in voltages, and stress distributions arising from the dielectric presence.

1.8 Scope of Thesis

The focus of this thesis will be on the simulation and modelling of MEMS cantilever beams which have a low pull-in voltage. This research will mainly focus on utilising COMSOL Multiphysics 6.2 which is a finite element analysis (FEA) software, to research the coupled electromechanical behaviour of the cantilever structure. The outline is as follows:

- **Theoretical Analysis:** Derivation and implementation of analytical models for prediction of the pull-in voltage of a cantilever beam in static (considering fundamental electrostatic and mechanical principles). The discussion will expand to the analysis of the stiffness of the beam, the deflection characteristics of the beam under load, and the coupling nature between the mechanical restoring forces and electrostatic actuation forces.
- **Numerical Simulation:** A model development, COMSOL Multiphysics 3D of a cantilever beam having an electrostatic actuator is the aim for this thesis. In this model, it will consider geometry, material properties, boundary conditions and Multiphysics coupling. The mechanical questions to consider include large deformations, stress distribution of the beam, and the mechanical response which leads to pull-in.
- **Parametric analyses:** A comprehensive study of the effects of significant geometric parameters (length, width, thickness of the cantilever and initial electrode gap between the beam and the stationary electrode) on pull-in voltage. Investigation of how variations of these variables affect the mechanical stiffness and compliancy of the cantilever and effect its deflection and pull-in behaviour is expected.

- **Validation of the Model:** By means of theoretical pull-in voltages computed using analytical models derived in Chapter 3, subsequently matched against simulation data, the correctness and robustness of the COMSOL model are validated. In order to understand the effects of geometry and dielectric layers, results are extensively investigated thus stressing trade-offs between device size, operating voltage, and mechanical stress and so guiding ideal MEMS switch design.

1.9 Related Works

The constraints on the design and performance of MEMS cantilever beams have changed drastically to meet the intended use of applications in a wide range of fields. The move towards miniaturization of system components, low-power consumption, and mechanical reliability has spurred new and innovative realizations for cantilever mechanics, i.e. applications where deflection, mechanical force sensitivity, mechanical fatigue resistance, and actuation voltage are crucial. The following are the highlighted application areas where the mechanical aspects of MEMS cantilever beams have had a direct impact on their design:

1.9.1 Biomedical Implants and Microvalves

MEMS cantilevers serve as particularly critical components within medical implant devices, where accuracy, reliability, and low-voltage operation are essential. Specifically, in implantable medical devices of microvalves for controlled drug delivery (for example, insulin pumps, high-frequency chemotherapy dispensers) the cantilever must deform, under electrostatic force, at low voltages while being subjected to the mechanical biological loads and properties of human organs. Mechanically, these cantilevers had to:

- Operate at extremely low voltages (1-5 V) minimizing battery drain.
- Use biocompatible materials such as silicon nitride or Parylene, where surface properties are selected for favourable mechanical flexibility and corrosion resistance.
- Be designed with geometries that promote stress minimization and reduce fatigue and wear over long-term use.

Example: The MEMS drug delivery microvalve by Debiotech SA is based on a dynamically compliant cantilever that closes and opens precisely with small actuation voltages to administer a dose of drug at great reliability for many years.

1.9.2 Aerospace and Defence Systems

MEMS cantilever-based switches and relays are essential components in satellites, missiles, and drones for a range of applications, including frequency tuning, micro-thrust control, structural health monitoring and other uses in between. As MEMS switch technology is developed for aerospace and defence systems, the systems will require the following:

- Designs that can withstand extreme vibrations to survive launch from a rocket and supersonic flight.
- Operational low pull-in voltages for power-constrained environments.
- High fatigue capacity, as switches may need to operate in extreme temperature cycles and withstand mechanical shock loads.

For example, RF MEMS switches may be used in phased array radar systems, cantilever beams with high stiffness but optimized damping allow for the maintenance of contact integrity while maintaining radio frequency switching.

1.9.3 Wearable Sensors and IoT Devices

MEMS accelerometers, gyroscopic sensors, accelerometers, pressure sensors (and other sensors) that are all found in wearable fitness trackers, smartphones, smartwatches etc., are designed using cantilever beams. Wearable devices must:

- Have the best sensitivity to energetic motion while also having good power characteristics. In many instances manufacturers will expect a device to operate on a coin cell battery while offering a response time less than a few seconds.
- These devices must withstand many cycles of repetitive mechanical loading from user motion and continuous vibrations from the environment.
- In order to investigate in real-time (and more directly) the activity of individuals wearables must be robust against common mechanical shocks from user (e.g., accidental drop).

In order to satisfy these users, manufacturers must design cantilevers that will have:

- Low stiffness, so that large deflections can be achieved while sensing with little energy, there are limits imposed by mechanical hysteresis and fatigue.
- Mechanical damping structures to prevent overshoot and resonance.
- Materials selection such as polysilicon just right for easy determination to provide a good mechanical compromise between stiffness and fatigue response.

Example: STMicroelectronics MEMS accelerometers today achieve high-performance sensing using suspended cantilever beams in a differential capacitive arrangement to measure user motion.

1.9.4 Environmental and Structural Monitoring

In the field of remote sensing and civil infrastructure monitoring, MEMS cantilevers are encompassed in a class of vibration and tilt sensors used for bridges, pipelines and buildings. Applications of MEMS cantilevers require, in various degrees,

- Durable mechanical function in an exterior environment (humidity, dust, temperature).
- Long-term reliability, often many years without required maintenance.
- Mechanical tuning to a desired frequency band of interest with respect to structural resonance.

For example, one type of vibration monitoring sensors embedded in railway tracks uses cantilever MEMS to measure micro-vibrations of deployed train loads. The cantilever structure is mechanically tuned to resonate in the relevant frequency range (e.g., 20 - 100 Hz) for suitable sensitivity and selectivity.

CHAPTER 2

LITRAURE REVIEW

The research of MEMS cantilever beams and the pull-in phenomenon has been an established trend in microelectromechanical systems research for decades. Early work primarily focused on developing analytical models to determine pull-in voltage for simple geometries.

2.1 Analytical Modelling of Pull-in Phenomenon

The fundamental science of electrostatic pull-in instability can be traced back to the early analysis of parallel-plate capacitors. The work of P. M. Osterberg and S. D. Senturia (1997) on electromechanical analysis of MEMS included the derivation of pull-in conditions for parallel-plate actuators [1]. Their work revealed the important "1/3 rule" which states that pull-in occurs when the movable electrode has deflected about one-third of the initial gap, that is there is a critical gap of 1/3 of the initial separation. This model of lumped-parameters, while a simplified application, was useful for initially predicting the pull-in voltage (V_{pi}) in terms of the mechanical stiffness and the electrostatic forces. For cantilever beams, the generalized nature of the electrostatic force and the continuously varying gap along the length of the beam require more complex approaches to analyse the system than simple lumped models. Mechanical modelling is based upon the Euler-Bernoulli beam theory that assumes plane sections remain plane and normal to the neutral axis, neglects shear deformations, and ignores rotary inertia, which is valid for slender beams [19]. Various researchers have used an array of techniques to solve the resulting small-deflection and non-linear differential equations. A popular method is the Galerkin method, that Senturia (2001) described [2], which has often been used to approximate the beam's deflection profile and produce more accurate analytical expressions for V_{pi} by converting the partial differential equation to a set of non-linear algebraic equations. These distributed models may reasonably account for the effects associated with the non-uniform electrostatic pressure and they yield deflection profiles that better match experimental results versus simple lumped models.

As an example, Maboudian and Howe (1997) reviewed the mechanical modelling of MEMS structures which included pull-in instability, and different analytical approximations for an assortment of beam geometries [8]. However, even though analytical models are available, they often represent simplified models that break down for certain geometries, neglect the effects of fringing fields, not consider large

deformation effects (geometric non-linearity), or consider the effects of residual stresses.[32]. When deflections are comparable to the thickness or length of the beam, non-linear beam theories (e.g., considering mid-plane stretching) become necessary to suitably capture the stiffening effect associated with the large deformations that apply a different and greater pull-in voltage than the pull-in voltage from linear beam theory [13, 41]. Furthermore, the inability to obtain closed-form solutions for advanced MEMS designs of complicated geometries and/or multi-layer beams further restrict the capabilities of the purely analytical approach [32].

2.2 Numerical Simulation Methods

The complexity of MEMS device geometries, the non-linearity of electrostatic forces, and the possible need for a reliable prediction of large elastic deflections outlined the acceptance of simulation methods, particularly Finite Element Analysis (FEA). R. K. Gupta (1997) and others initiated the demonstration of FEA methods for MEMS devices by demonstrating its utility with complex designs and coupled physics phenomena [3].

2.2.1 Full Field Analysis and Mechanical Response:

COMSOL will permit full field analysis of electric fields within the structure and indeed the stress with strain and deformation of the entire structure which would be difficult to obtain from an analytical model. This gives an opportunity to see where stress concentrations occur, particularly at the anchor regions of the cantilever where mechanical stress is likely to be highest, and to work on device reliability [11]. Full field analysis is critical for predicting long-term performance of a device and to avoid premature failure as a result of fatigue or fracture. The 3-D visualization of deformation will represent novel qualitative and quantitative information of the mechanical response of the beam at elastic loading.

2.2.2 Geometric and Material Parameters Sweeping:

The capability for parametric sweep offered by the software will make it possible to systematically study the change in pull-in voltage as well as overall performance of the device as each geometric parameter (length, thickness, gap, etc.) and material properties are varied one at a time. This parametric study could lead to a rapid design optimization, as it has been performed in other studies, to fit a precise voltage threshold and a desired dynamic behaviour [12].

2.3 The Critical Role of Dielectric Interface

Not only are dielectric layers passive insulators, but they also are fundamental for the performance, long-term dependability, and functioning of both capacitive and ohmic MEMS switches. Their main goals include:

- Electrical isolation: Specifically in capacitive switches where direct contact might cause device failure, prevent short connections between the moveable beam and the actuation electrode.
- Anti-Stiction Properties: Offering a surface with less surface energy than metal-to-metal contact, hence lowering adhesion forces (e.g., van der Waals forces, capillary forces) and so addressing the ubiquitous stiction problem whereby the beam becomes permanently stuck after actuation [7].

In capacitive switches, the thickness and dielectric constant of the dielectric layer directly affect the ON-state capacitance of the switch.

A commonly used dielectric material in MEMS is silicon nitride (Si_3N_4), which offers convergence of desirable features. It is compatible, showing outstanding electrical insulation with a high dielectric strength (usually $> 10 \text{ MV/cm}$), robust mechanical stability (high Young's modulus), good thermal stability, and chemical inertness.

But the existence of a dielectric layer presents a different set of major problems mostly related to dielectric charging. This phenomenon generates residual electric fields by the injection and subsequent trapping of charges inside the dielectric substance. Fowler-Nordheim tunnelling (at high electric fields), Poole-Frenkel emission, or direct injection from the contacting electrodes can all be components of charge injection mechanisms. These charges become trapped in localised energy levels (trap states) within the bandgap of the dielectric once injected. This accumulated charge modulates the effective electric field across the gap, hence changing the electrostatic force applied on the moveable beam [9]. In 2012, Wang and Li undertook an extensive simulation investigation on how dielectric charging affected MEMS switch long-term dependability. Their experiment showed how well trapped charges close the electrostatic gap, hence lowering the pull-in voltage over time. This voltage change can greatly affect device lifetime and performance by either causing the switch to actuate early or fail to release [10]. Moreover, dielectric charging can cause hysteresis in the pull-in/release voltage characteristics, in which case the release voltage gets much lower than the pull-in voltage and occasionally causes permanent stiction. Predicting and reducing these dependability problems depends on

accurate modelling of charge transport and trapping mechanisms, usually requiring specialised physics interfaces or bespoke equations inside COMSOL.

2.4 Strategies to Lower Pull-in Voltage

With an eye toward mechanical design, studies on lowering pull-in voltage have investigated several strategies often drawing on ideas from both analytical models and numerical simulations:

2.4.1 Geometric optimization:

- **Stiffness and dimensions of beams:** Pull-in voltage of the cantilever beam depends on its mechanical stiffness. The easiest approaches to lower the stiffness of the cantilever beam and, hence, the pull-in voltage [2, 6] are increasing its length (L) and thickness (h). Examining these fundamental correlations, M. J. Madou (2011) and F. E. H. Tay (2002) show how the cube of the length and the square root of the thickness [6, 5] determine the pull-in voltage. Because the moment of inertia (I) depends on the cube of the thickness (h^3), a little decrease in thickness usually produces a clear decrease in stiffness. Although its effect is less obvious than that of changes in length or thickness, increasing width (b) adds to the actuation area, so helping to reduce pull-in. Extending the length, on the other hand, can slow response times and increase the device's stictional susceptibility. Thinner designs run the danger of losing mechanical strength, can complicate manufacturing, and are more sensitive to environmental shocks or vibrations.
- **Smaller First Gap (g_0):** Shorter distances the beam moves to reach the pull-in point by means of a smaller gap between the beam and the electrode. This reduces the need of mechanical restoring force. It hence requires less electrostatic force, which lowers VPI [5]. In MEMS switches and RF devices, engineers apply this concept [12]. Van der Waals forces take over when the gap gets very small, hence stiction also becomes more likely [15]. One typical problem in MEMS design is balancing low pull-in with stiction. Often this requires anti-stiction coatings or particular design modifications to prevent parts from sticking together.

Materials chosen and mechanical behaviour understood relate to a property known as Young's modulus (E). This characteristic reveals the stiffness of a beam. More flexible structures result from a material having a smaller Young's modulus. It reduces the pull-in

voltage in case the geometry remains the same. Single-crystal silicon's great mechanical properties—strong strength and durability under repeated stress—have engineers choosing it. It also fits very nicely with conventional CMOS manufacturing methods. Its increasing Young's modulus increases pull-in voltage. Researchers have looked at using polymers like SU-8 and Parylene or some forms of silicon nitride in order to address this issue. Usually referred to as "soft MEMS," these materials are more flexible because their Young's modulus is lower. In flexible electronics or bio-MEMS applications, they open possibilities and help to lower actuation voltages. For Parylene-based MEMS, for instance, studies show much lower pull-in voltages than silicon, although this often comes at the expense of mechanical durability thermal performance, or lasting reliability. Because of elements like grain size and deposition technique as well as built-up internal stresses, thin films can act from bulk materials. Measuring the mechanical characteristics of thin films will help one to replicate these structures.

2.5 Advanced Modelling and Performance Optimization

Recent studies have stretched MEMS switch modelling's limits beyond static pull-in analysis to encompass advanced optimisation techniques and more intricate dynamic events. Comprehensive knowledge of the dynamic response of the switch including its switching speed, transient contact behaviour, and the consequences of damping depends on time-dependent simulations. To examine the impact dynamics of a gold beam striking a dielectric-coated electrode, Johnson et al. (2017) undertook transient electromechanical simulations in COMSOL. Their work gave important new perspectives on events such as contact bouncing, settling durations, and the effect of several damping systems (e.g., structural damping, squeezing film damping from the air gap) on the general switching speed and stability [15]. Reasonable dynamic predictions depend on accurate damping models.

Moreover, major work has been done to maximise MEMS switch design parameters by means of parametric studies and sensitivity analysis. Researchers methodically investigate on important performance criteria the effects of geometric parameters (e.g., beam length, width, thickness, starting gap, electrode overlap) and material qualities. These criteria for RF MEMS switches span pull-in voltage and contact force to include isolation, return loss, and insertion loss. Although most of the current work has been on optimising either a limited set of coupled parameters or individual parameters, the complex interaction between mechanical design, electrostatic actuation, and the particular

characteristics of the dielectric interface remains an active and challenging topic of investigation. Above all, developing strong models that can forecast long-term dependability under different running conditions—including the combined impacts of dielectric charge and contact degradation—is critical. Often included into COMSOL's Optimisation Module, advanced optimisation methods can be used for multi-objective optimisation, balancing competing performance criteria (e.g., low pull-in voltage vs strong contact force).

CHAPTER 3

METHODOLOGY

3.1 Introduction

This chapter explains the modelling and simulation of MEMS cantilever beam switches. The goal was to set up a realistic simulation in COMSOL Multiphysics showing how these switches operate under different conditions. The study focuses on how the structure size and the dielectric layers influence the device's performance paying attention to pull-in voltage, motion, and electric field patterns. Studied two beam setups, one using larger beams and electrodes and the other using smaller ones. They ran simulations on both setups with and without adding a dielectric layer on the bottom electrode. This allowed them to see how having the dielectric layer changes how the switch behaves.

3.2 Software and Physics Interface

Modelled and simulated using COMSOL Multiphysics 6.2. This platform for finite element analysis performs effectively to solve problems involving several physics systems. Two main physics interfaces shaped the work:

- Solid Mechanics belonging to the Structural Mechanics Module investigated how the cantilever beam deforms due to electrostatic forces; Electrostatics from the AC/DC Module helped in simulating the distribution of the electric field and calculating the electrostatic force acting between the beam and the electrodes.
- Coupling these two modules through the Electromechanical Force Multiphysics Coupling let the structure bend from electrostatic pressure and let the deformation change the electrostatic field. This interaction operated in both directions.

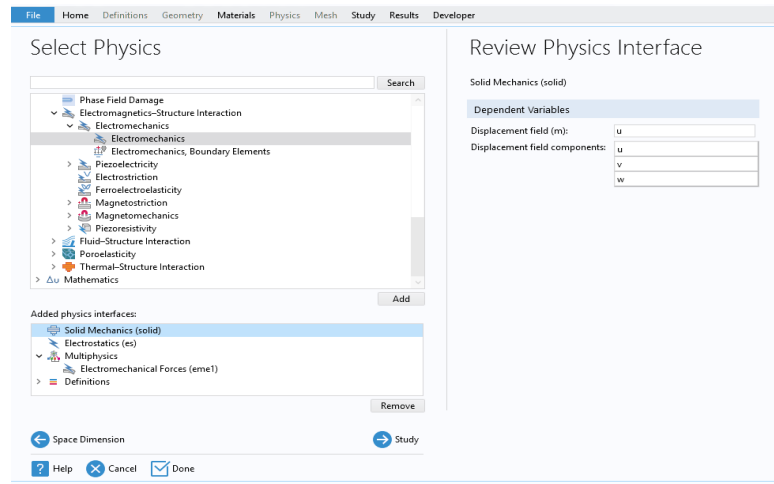


Figure 3.1 Selection of Physics

3.3 Geometric Modelling

Examined how structural parameters affect switch behaviour by creating two geometric setups:

3.3.1 Configuration A (Larger beam and electrode):

Size and Shape	Size and Shape
Width: 250 μm	Width: 130 μm
Depth: 130 μm	Depth: 130 μm
Height: 1.5 μm	Height: 0.5 μm
Position	Position
Base: Corner	Base: Corner
x: 0 μm	x: 0 μm
y: 0 μm	y: 0 μm
z: 0 μm	z: -2 μm
Axis	Axis
Axis type: z-axis	Axis type: z-axis

Figure 3.2 Configuration of Larger beam and electrode respectively

The air gap was 2 μm .

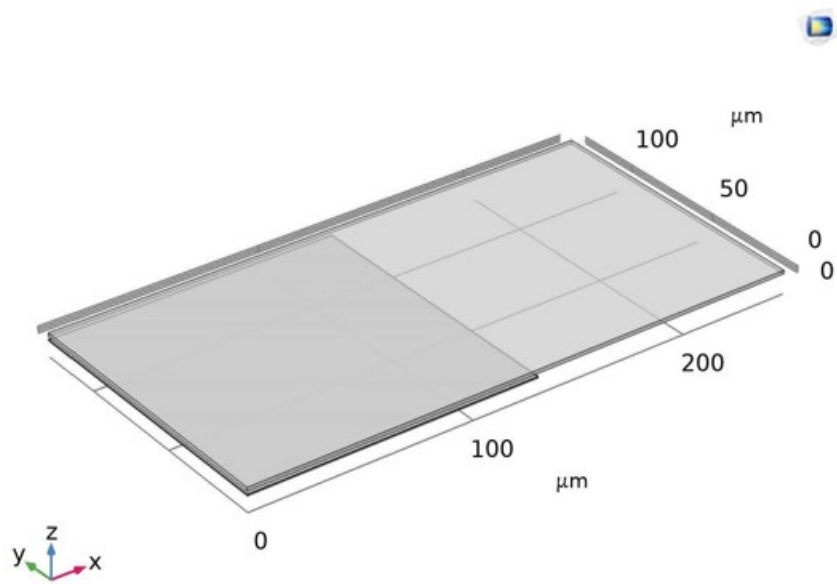


Figure 3.3 Geometry of Configuration A

3.3.2 Configuration B (Smaller beam and electrode):

Size and Shape	Size and Shape
Width: 140 μm	Width: 75 μm
Depth: 75 μm	Depth: 75 μm
Height: 1.5 μm	Height: 0.5 μm
Position	Position
Base: Corner	Base: Corner
x: 0 μm	x: 0 μm
y: 0 μm	y: 0 μm
z: 0 μm	z: -2 μm
Axis	Axis
Axis type: z-axis	Axis type: z-axis

Figure 3.4 Configuration of Smaller beam and electrode respectively

The air gap is 2 μm.

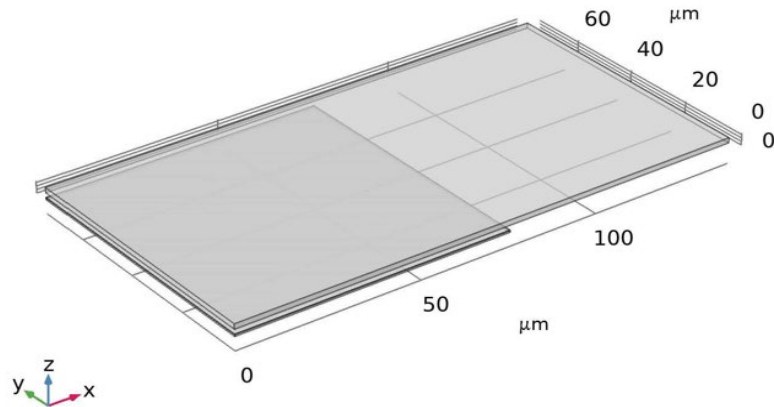


Figure 3.5 Geometry of Configuration B

Examined each setup in two types:

- One without any dielectric layer.
- One with a dielectric layer made of silicon nitride, 0.15 μm thick, and with a relative permittivity of 9.7. This layer is located above the bottom electrode.

3.4 Material Properties

The material selection is critical for accurate simulation. The following materials were used:

Table 3.1 Summary Material Properties

Component	Material	Young's Modulus (GPa)	Density (kg/m ³)	Electrical Conductivity (S/m)	Relative Permittivity (ϵ_r)	Poisson's Ratio
Cantilever Beam	Gold	78	19300	4.1×10^7	1	0.44
	Polysilicon	160	2320	1×10^{-3}	1	0.22
Electrode	Gold	78	19300	4.1×10^7	1	0.44
	Copper	110	8960	5.8×10^7	1	0.34
	Aluminium	70	2700	3.7×10^7	1	0.33
Dielectric Layer	Silicon Nitride	250	3100	1×10^{-14}	9.7	0.27

3.5 Boundary Conditions and Electrical Loading

To accurately represent a cantilever beam in COMSOL:

3.5.1 Solid Mechanics

- Fixed the anchor end of the cantilever and the bottom electrode to keep displacement at zero in every direction.
- The cantilever tip was allowed to deform.
- The rest of the beam could move as electrostatic forces acted on it.

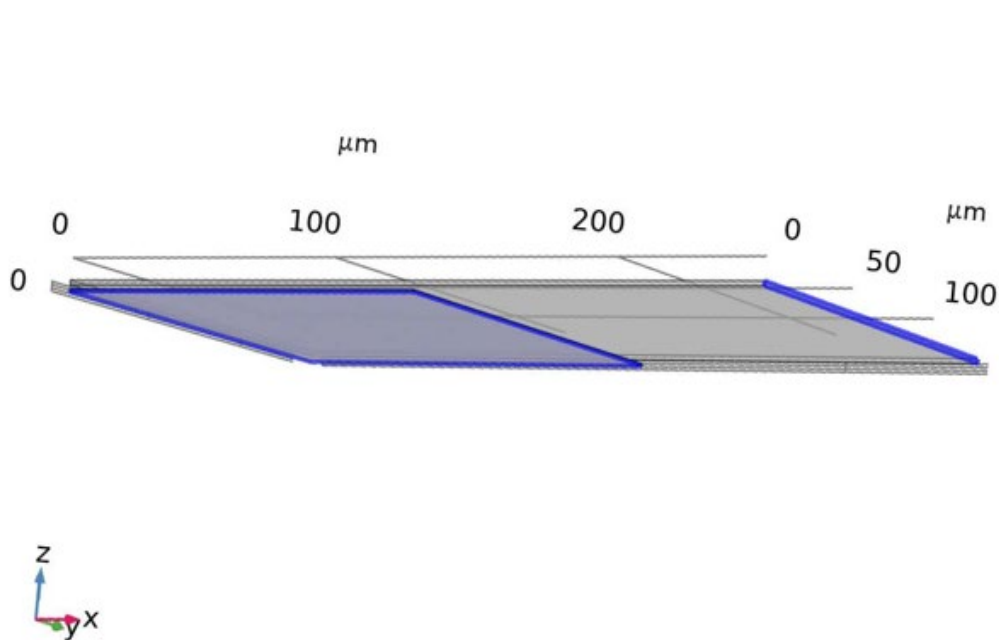


Figure 3.6 Fixed Constraints

3.5.2 Electrostatics

- A voltage adjusted through a parametric sweep ranging from 0 to 5V, 0 to 10V, or 0 to 20V, was applied to the bottom electrode.
- The beam was grounded (0V).
- If a dielectric layer was included, its permittivity was defined.

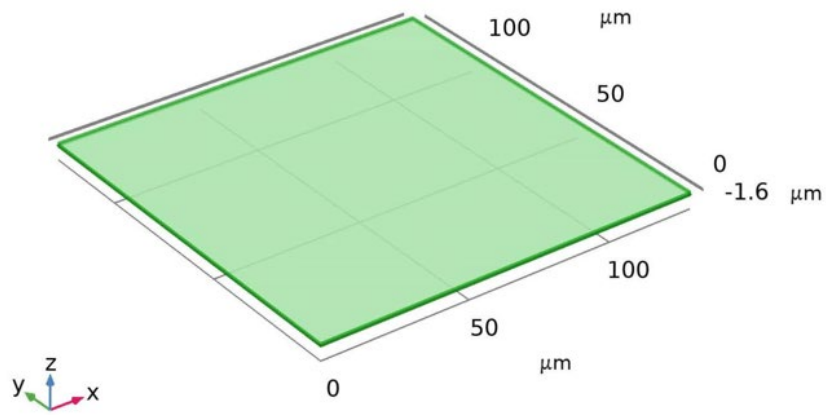


Figure 3.7 Applied Voltage on Electrode

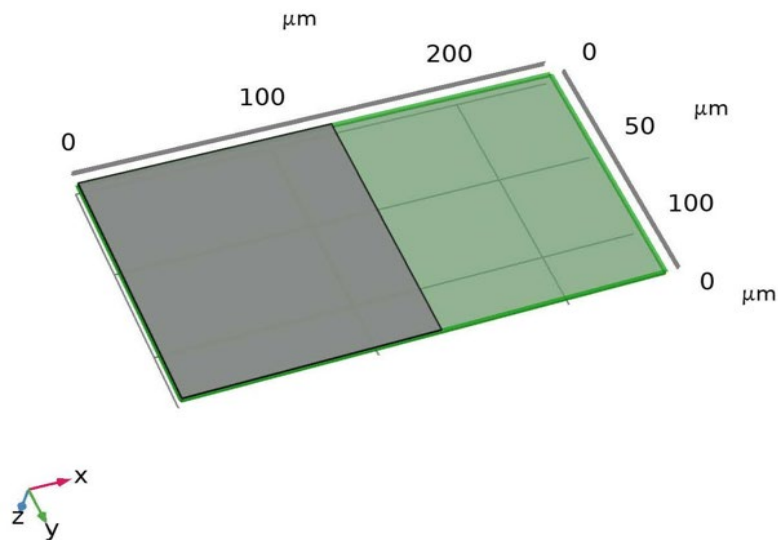


Figure 3.8 Grounded Beam

3.5.3 Multiphysics Integration

This built-in coupling links the deformation projected by solid mechanics with the electrostatic forces calculated by the electrostatics module automatically. It guarantees bidirectional feedback since the electric field and capacitance change as the beam deflects, so influencing the electrostatic forces and hence displacement. Pull-in instability can be properly captured only with this nonlinear feedback loop.

3.6 Mesh Configuration

Implemented a physics-based meshing approach in COMSOL Multiphysics to get robust and precise numerical outcomes when modelling MEMS cantilever structures. They used tiny mesh configurations to capture minute features such as variations in the electric field due to deformation and electromechanical interactions surrounding the beam-electrode gap and the beam's anchorage locations.

3.6.1 Meshing Type and Control Settings

- Mesh Type: Physics-Controlled Mesh
- Element Size Setting: Fine
- Element Type: Tetrahedral for 3D domains
- Boundary Layer Mesh: Applied near dielectric surfaces and gap regions

3.6.2 Refinements:

- Extra fine elements were added at the beam tip and at the edges of the electrodes to boost detail in areas with steep gradients.
- Local element size:
 - Minimum Element Size: Around $0.405\ \mu\text{m}$
 - Maximum Element Size: $9.45\ \mu\text{m}$
 - Curve Factor: 0.3

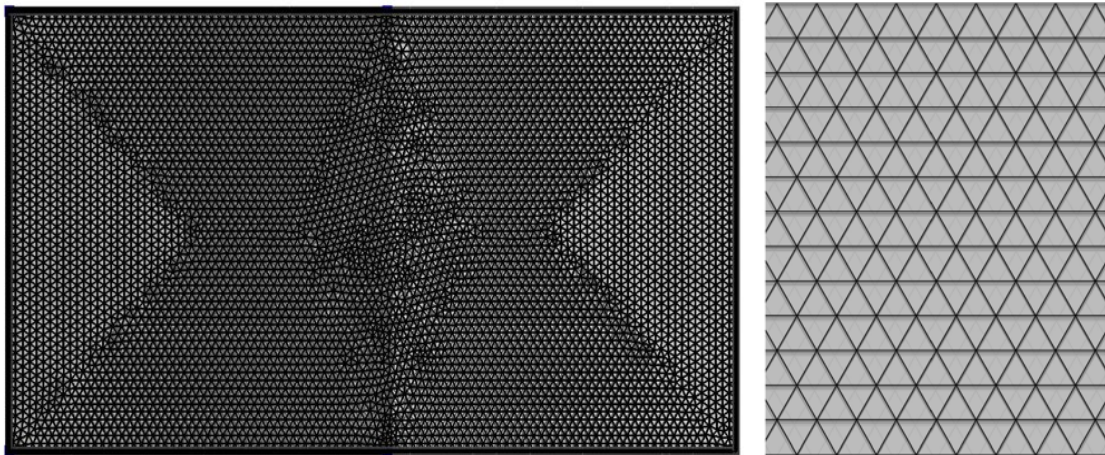


Figure 3.9 Meshing

3.7 Analytical Pull-in Voltage Estimation

Pull-in Voltage (V_{pi}) is the voltage at which the electrostatic force exceeds the restoring force of the cantilever, and thus leads to an unstable condition in which the

cantilever collapses to the fixed electrode.[10] The pull-in usually occurs when the gap has decreased to approximately two-thirds to one-half of the original gap value.[8] (V_{pi}) denotes a limit of operation; exceeding (V_{pi}) may result in undesired performance failures through stiction or shorting. It certainly is necessary to make an accurate prediction of (V_{pi}) for an effective design.[7] A low (V_{pi}) is advantageous for low power consumption, and compatibility with standard CMOS circuitry, especially in portable devices. [13] In devices where pull-in is the desired actuation modality, such as switches, it is important to have a precise control over (V_{pi}) and to also be vigilant about the contact mechanics and reliability issues presented.[2]

3.7.1 Pull-in Voltage without Dielectric Layer

For a cantilever beam-type capacitive switch, the pull-in voltage can be approximated using the following formula:

$$V_{Pi} = \sqrt{\frac{8K_{eq}g_0^3}{27\epsilon_0 A_{eff}}} \quad (3.1)$$

Where:

- V_{pi} : Pull-in voltage
- K_{eq} : Equivalent Spring constant of the cantilever beam
- g_0 : Initial air gap between beam and electrode
- $\epsilon_0 = 8.854 \times 10^{-12}$ F/m: Permittivity of free space
- A_{eff} : Overlapping area between the beam and the bottom electrode

The equivalent spring constant k_{eq} for a rectangular cantilever beam is given by:

$$K_{eq} = \frac{3EI}{L^3} \quad \text{with} \quad I = \frac{bh^3}{12} \quad (3.2)$$

Where:

- E : Young's modulus of the beam material
- I : Area moment of inertia
- b : Width of the beam
- h : Thickness of the beam
- L : Length of the beam

3.7.2 Pull-in Voltage with Dielectric Layer

In configurations where a dielectric layer is present above the bottom electrode (such as silicon nitride), the effective capacitive gap increases due to the reduced electric field across the dielectric. The effective gap g_{eff} is modified as:

$$g_{\text{eff}} = g_0 + \frac{t_d}{\epsilon_r} \quad (3.3)$$

Where:

- t_d : Thickness of the dielectric layer
- ϵ_r : Relative permittivity of the dielectric material

The modified pull-in voltage becomes:

$$V_{\text{Pi}} = \sqrt{\frac{8K_{eq}g_{\text{eff}}^3}{27\epsilon_0\epsilon_r A_{\text{eff}}}} \quad (3.4)$$

This formula accounts for the reduced electrostatic coupling due to the dielectric interface, which generally increases the pull-in voltage.

3.7.3 The 1/3 Rule and Pull-in Instability

The analytical model also relies on a fundamental result known as the “1/3 rule.” This states that pull-in occurs when the beam deflects by one-third of the initial air gap, i.e.,

$$x_{\text{pull-in}} = \frac{g_0}{3} \quad (3.5)$$

At this critical deflection, the system becomes unstable because the electrostatic force increases faster than the restoring mechanical force, leading to sudden snap-down of the beam to the electrode. This is a key stability criterion in MEMS device design and is inherently captured in the derivation of the pull-in voltage formula.

3.8 Study and Solver Settings

The simulations were set up using a stationary parametric study to observe the beam's static deformation under increasing voltages. Key settings include:

- Voltage Sweep Range: (0 V to 5 V) or (0V to 10V) or (0V to 20V)
- Increment: 0.1 V or 0.5V or 1V
- Solver: Fully coupled, direct solver for higher accuracy

The Electromechanical Force Coupling ensured that the electrostatic forces and structural deformation were solved simultaneously at each voltage step.

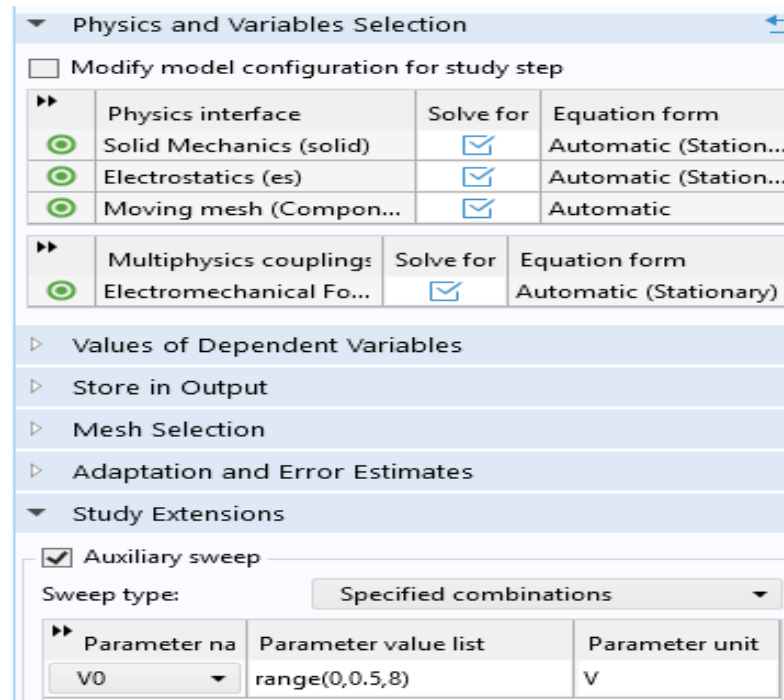


Figure 3.10 Showing solver parameters and convergence settings

3.9 Simulation Cases and Evaluation Metrics

To enable a comparative study of various design configurations, eleven simulation cases were set up based on beam dimensions and presence or absence of a dielectric layer.

For each simulation case, the following key parameters were recorded for later analysis:

- Displacement at the beam tip
- Voltage at which pull-in instability occurs
- Distribution of the electric field across the gap
- Von Mises stress distribution along the beam

Table 3.2 Overview of Simulation Cases

Combo ID	Beam Material	Beam Dimensions (μm)	Electrode Material	Electrode Dimensions (μm)	Dielectric Layer	Dielectric Dimensions (μm)
C1	Gold	$250 \times 130 \times 1.5$	Aluminium	$130 \times 130 \times 0.5$	Yes	$130 \times 130 \times 0.15$
C2	Gold	$140 \times 75 \times 1.5$	Aluminium	$75 \times 75 \times 0.5$	Yes	$75 \times 75 \times 0.15$
C3	Gold	$250 \times 130 \times 1.5$	Copper	$130 \times 130 \times 0.5$	Yes	$130 \times 130 \times 0.15$
C4	Gold	$140 \times 75 \times 1.5$	Copper	$75 \times 75 \times 0.5$	Yes	$75 \times 75 \times 0.15$
C5	Gold	$140 \times 75 \times 1.5$	Copper	$75 \times 75 \times 0.5$	No	—
C6	Polysilicon	$250 \times 130 \times 1.5$	Aluminium	$130 \times 130 \times 0.5$	Yes	$130 \times 130 \times 0.15$
C7	Polysilicon	$140 \times 75 \times 1.5$	Aluminium	$75 \times 75 \times 0.5$	Yes	$75 \times 75 \times 0.15$
C8	Polysilicon	$140 \times 75 \times 1.5$	Aluminium	$75 \times 75 \times 0.5$	No	—
C9	Polysilicon	$250 \times 130 \times 1.5$	Gold	$130 \times 130 \times 0.5$	Yes	$130 \times 130 \times 0.15$
C10	Polysilicon	$140 \times 75 \times 1.5$	Gold	$75 \times 75 \times 0.5$	Yes	$75 \times 75 \times 0.15$

CHAPTER 4

RESULTS AND DISCUSSION

4.1 Introduction

This chapter carefully analyses the simulation results for MEMS cantilever beam-type capacitive switches modelled in COMSOL Multiphysics. Ten scenarios with different beam size and dielectric layer presence were explored to find their impacts on structural stress, pull-in voltage, electric field distribution, and tip displacement. The results enable the understanding of the electromechanical behaviour of the switches, hence guiding optimisation for practical MEMS applications.

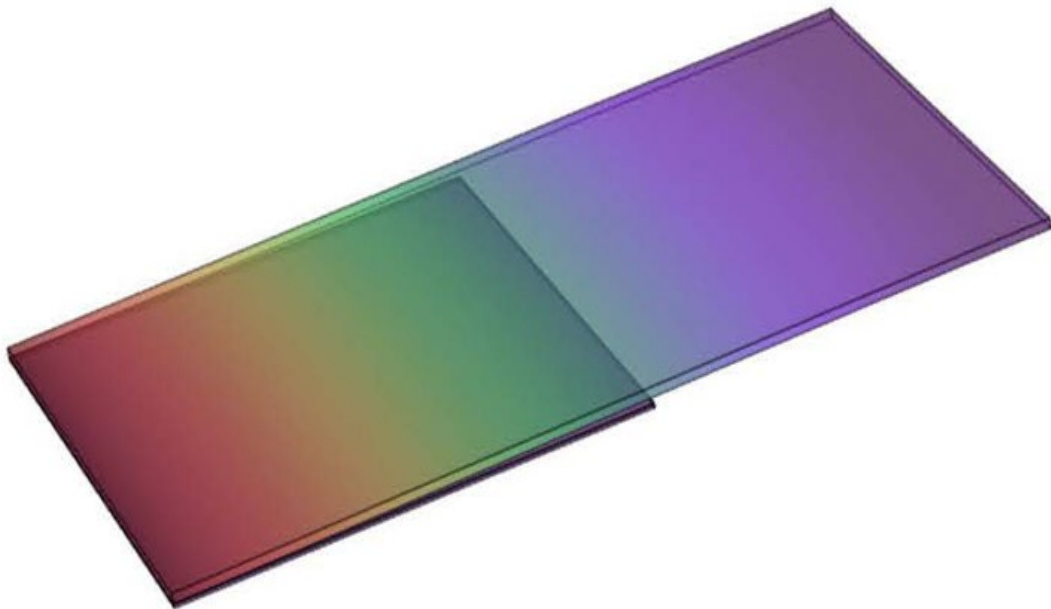


Figure 4.1 Bending of Beam

4.2 Tip Displacement vs Voltage Behaviour

The displacement of the cantilever beam tip was monitored under a voltage sweep from 0V to 10V. The relationship between tip displacement and applied voltage was nonlinear due to the electrostatic force increasing quadratically with voltage, balanced by the mechanical restoring force of the beam.

4.2.1 Case C1 (Gold, Bigger Beam, Al Electrode, With Layer)

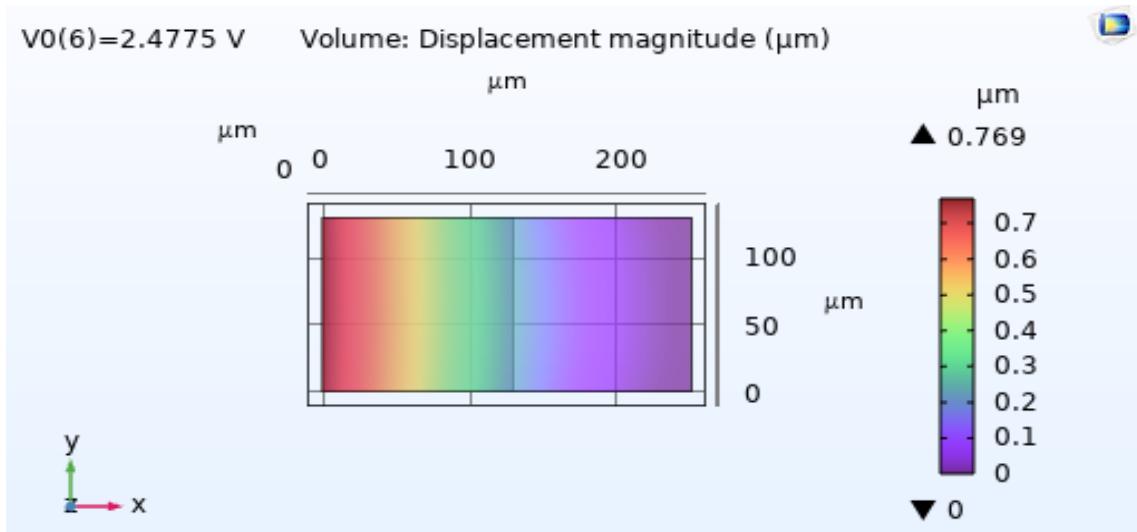


Figure 4.2 Beam Displacement Behaviour of C1

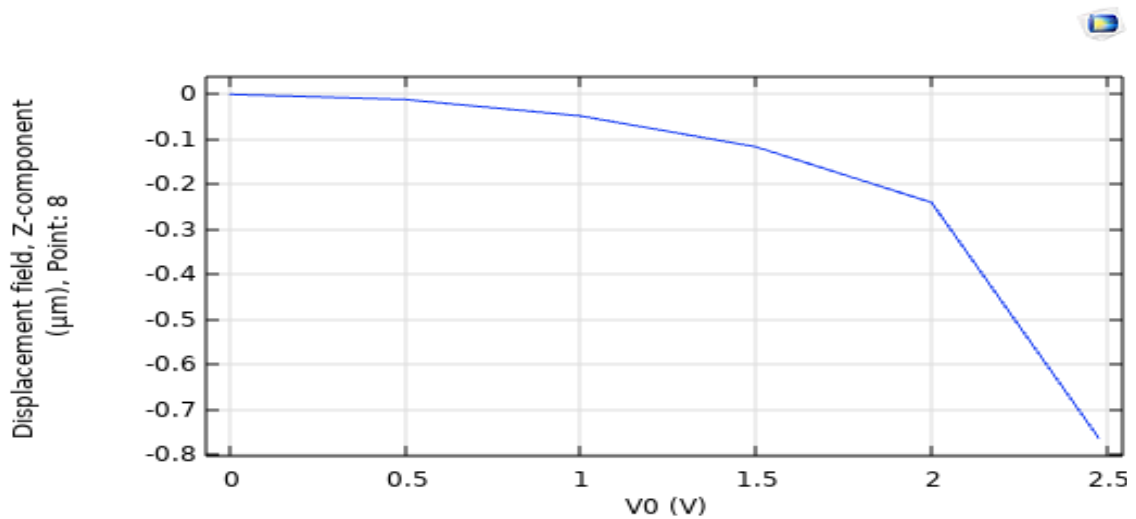


Figure 4.3 Beam Displacement VS Voltage Graph of C1

Table 4.1 Displacement Field VS Voltage Table of C1

V0 (V)	Displacement field, Z-component (μm), Point: 8
0.0000	0.0000
0.50000	-0.011537
1.0000	-0.048000
1.5000	-0.11656
2.0000	-0.23997
2.4775	-0.76390

4.2.2 Case C2 (Gold, Smaller Beam, Al Electrode, With Layer)

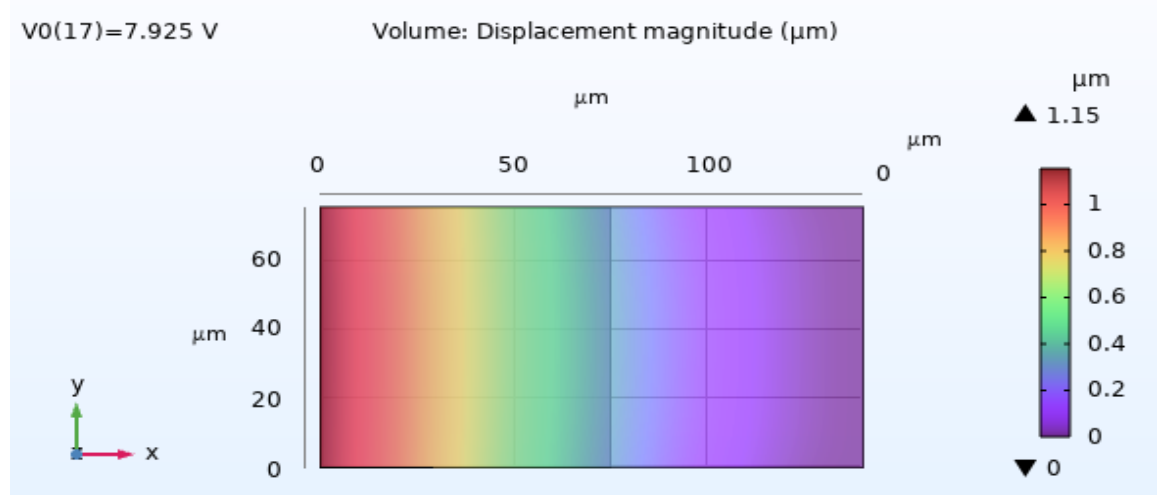


Figure 4.4 Beam Displacement Behaviour of C2

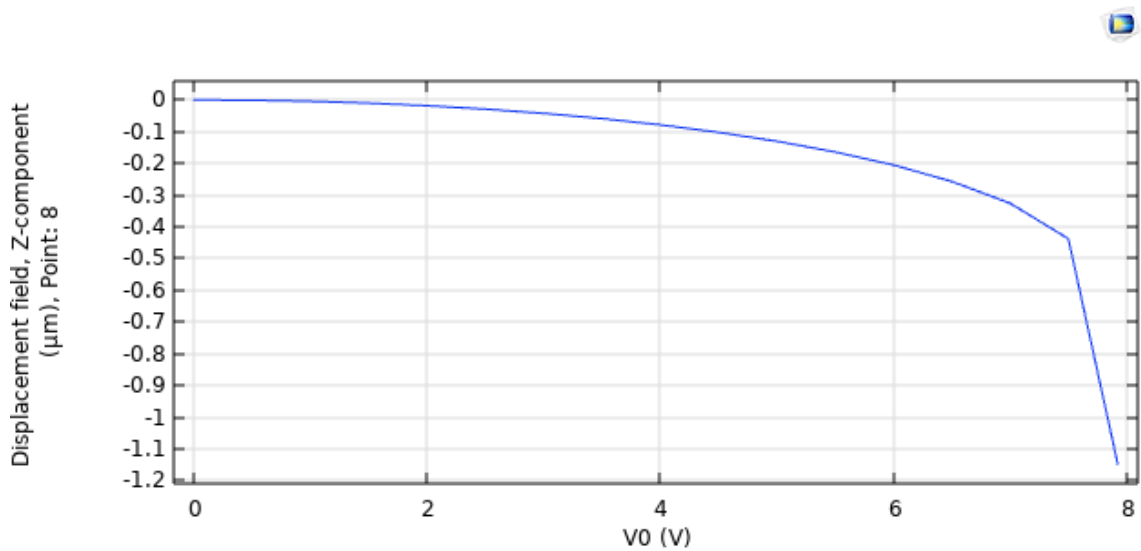


Figure 4.5 Beam Displacement VS Voltage Graph of C2

Table 4.2 Displacement Field VS Voltage Table of C2

V0 (V)	Displacement field, Z-component (μm), Point: 8
0.0000	0.0000
0.50000	-0.0011305
1.0000	-0.0045384
1.5000	-0.010273
2.0000	-0.018422
2.5000	-0.029112
3.0000	-0.042523

3.5000	-0.058971
4.0000	-0.078729
4.5000	-0.10232
5.0000	-0.13045
5.5000	-0.16421
6.0000	-0.20532
6.5000	-0.25692
7.0000	-0.32592
7.5000	-0.43769
7.9250	-1.1504

4.2.3 Case C3 (Gold, Bigger Beam, Cu Electrode, With Layer)

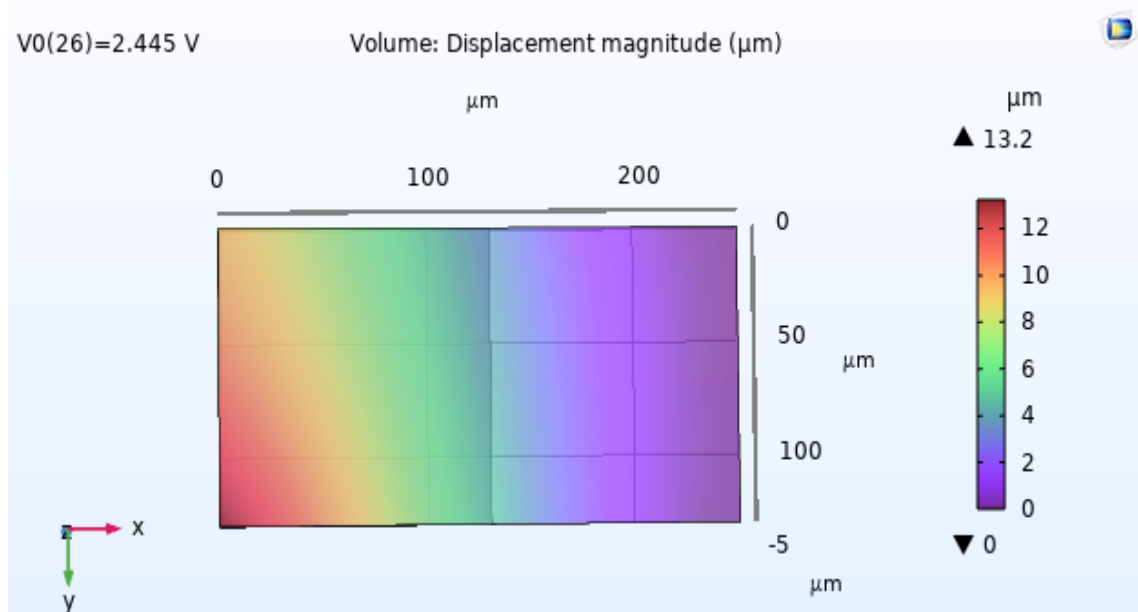


Figure 4.6 Beam Displacement Behaviour of C3

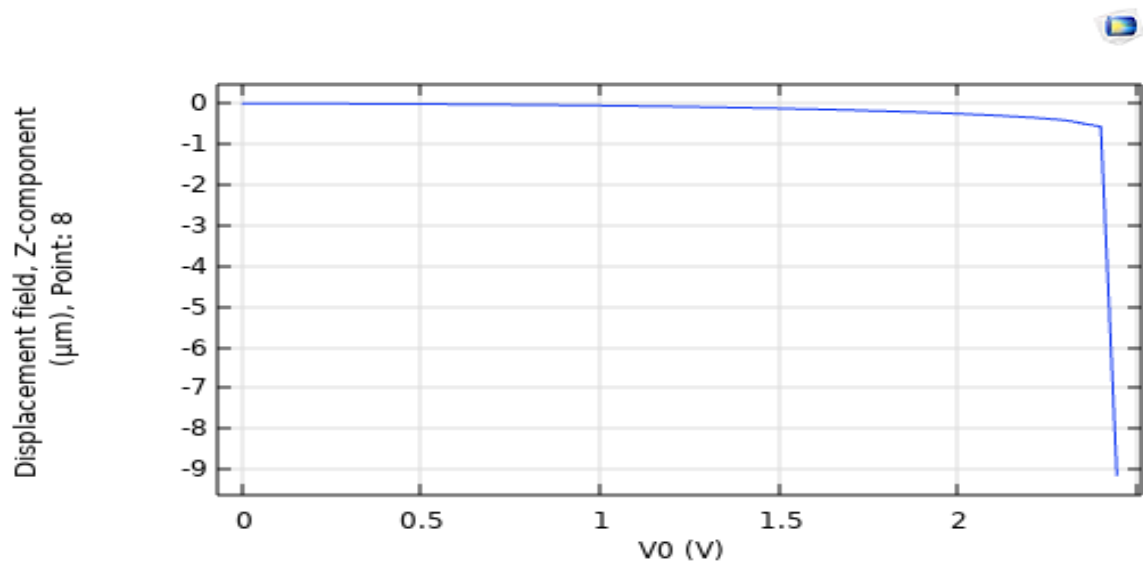


Figure 4.7 Beam Displacement VS Voltage Graph of C3

Table 4.3 Displacement Field VS Voltage Table of C3

V0 (V)	Displacement field, Z-component (μm), Point: 8
0.0000	0.0000
0.10000	-4.6680E-4
0.20000	-0.0018700
0.30000	-0.0042180
0.40000	-0.0075251
0.50000	-0.011812
0.60000	-0.017105
0.70000	-0.023440
0.80000	-0.030861
0.90000	-0.039419
1.0000	-0.049181
1.1000	-0.060226
1.2000	-0.072651
1.3000	-0.086576
1.4000	-0.10237
1.5000	-0.11990
1.6000	-0.13957

1.7000	-0.16173
1.8000	-0.18686
1.9000	-0.21568
2.0000	-0.24923
2.1000	-0.28936
2.2000	-0.33964
2.3000	-0.40970
2.4000	-0.56952
2.4450	-0.91631

4.2.4 Case C4 (Gold, Smaller Beam, Cu Electrode, With Layer)

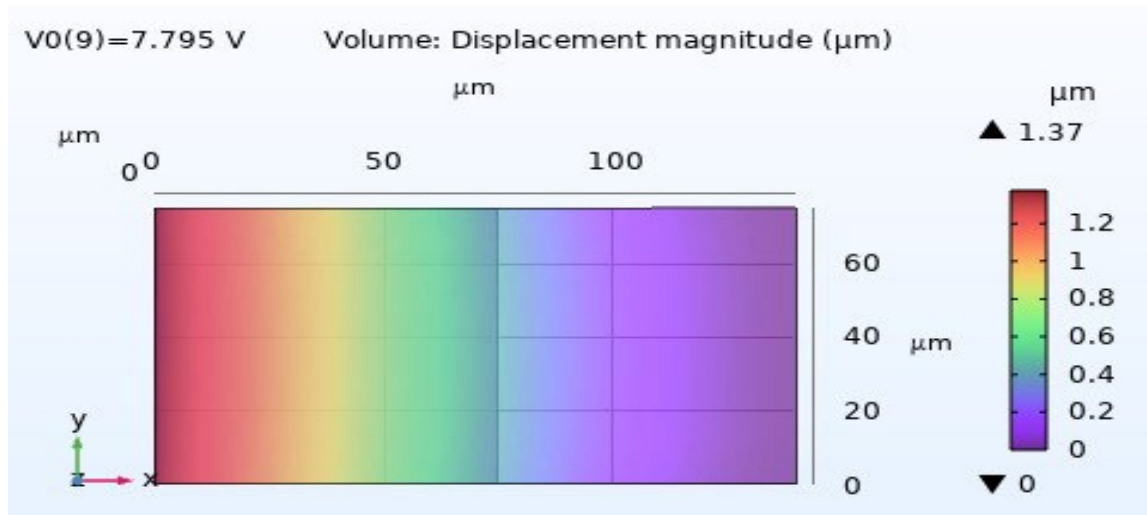


Figure 4.8 Beam Displacement Behaviour of C4

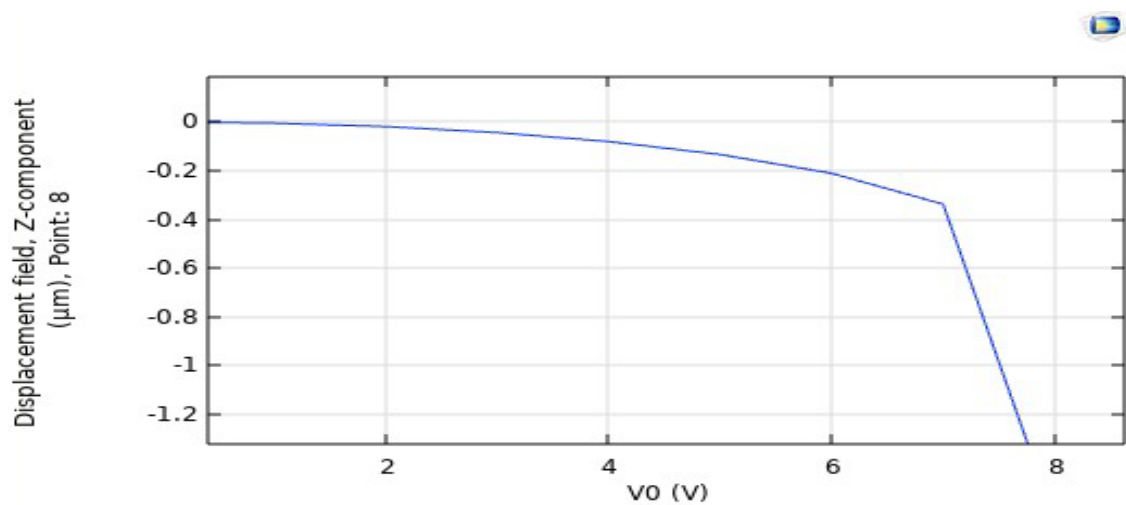


Figure 4.9 Beam Displacement VS Voltage Graph of C4

Table 4.4 Displacement Field VS Voltage Table of C4

V0 (V)	Displacement field, Z-component (μm), Point: 8
0.0000	0.0000
1.0000	-0.0046213
2.0000	-0.018761
3.0000	-0.043305
4.0000	-0.080314
5.0000	-0.13331
6.0000	-0.21049
7.0000	-0.33736
7.7950	-1.3687

4.2.5 Case C5 (Gold, Smaller Beam, Cu Electrode, No Layer)

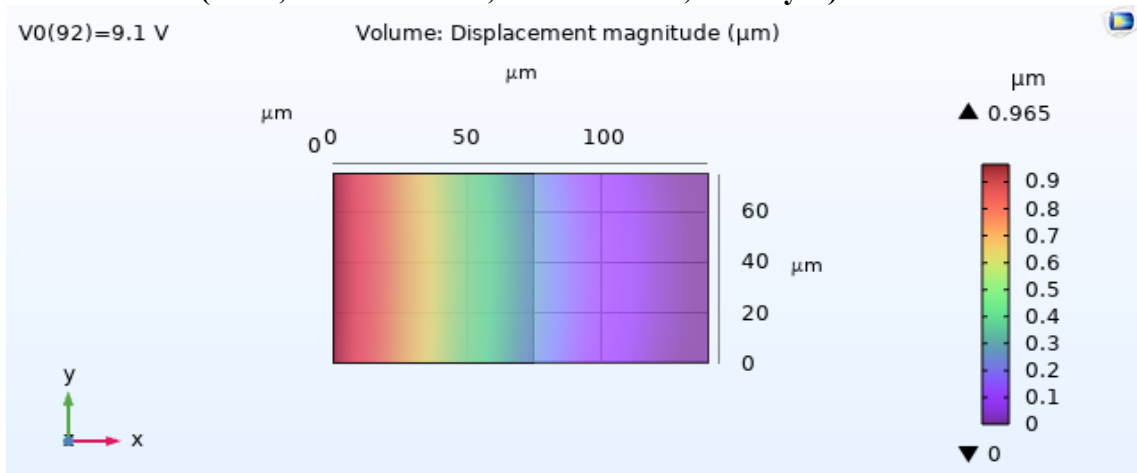


Figure 4.10 Beam Displacement Behaviour of C5

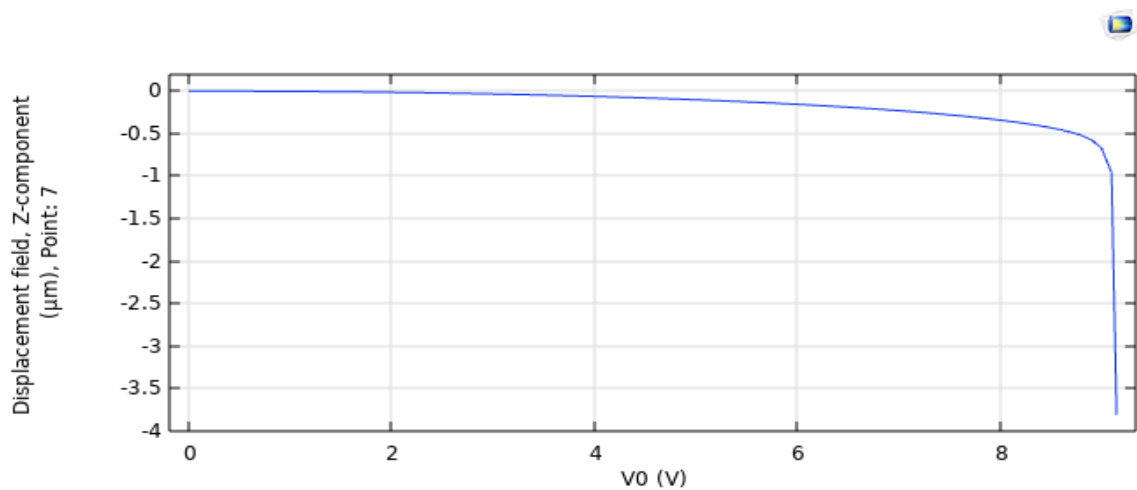


Figure 4.11 Beam Displacement VS Voltage Graph of C5

Table 4.5 Displacement Field VS Voltage Table of C5

V0 (V)	Displacement field, Z-component (μm), Point: 7
0	0.000
1.000	-0.0037277
2.000	-0.015075
3.000	-0.034564
4.000	-0.063197
5.000	-0.10272
6.000	-0.15626
7.000	-0.23061
8.000	-0.34238
9.000	-0.66860
9.150	-3.8090

4.2.6 Case C6 (Polysilicon, Bigger Beam, Al Electrode, With Layer)

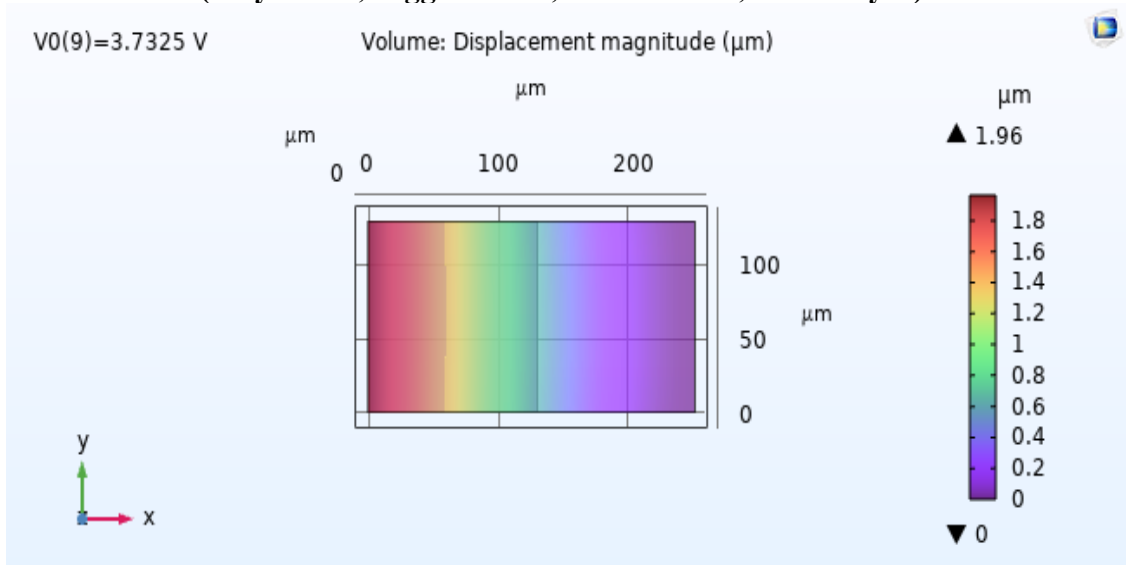


Figure 4.12 Beam Displacement Behaviour of C6

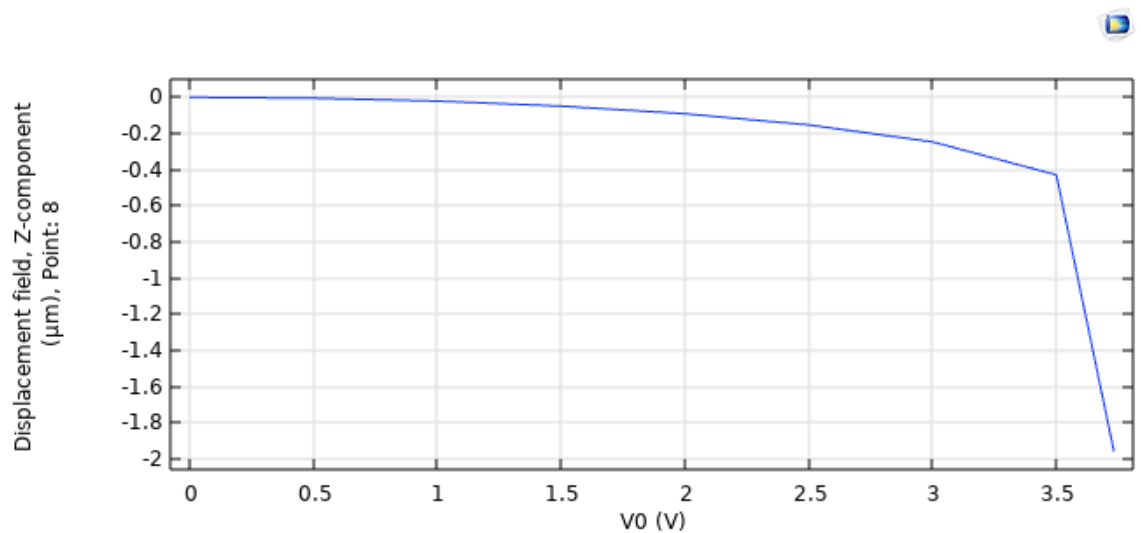


Figure 4.13 Beam Displacement VS Voltage Graph of C6

Table 4.6 Displacement Field VS Voltage Table of C6

V0 (V)	Displacement field, Z-component (μm), Point: 8
0.0000	0.0000
0.50000	-0.0051935
1.0000	-0.021121
1.5000	-0.048907
2.0000	-0.091241
2.5000	-0.15298
3.0000	-0.24662
3.5000	-0.42931
3.7325	-1.9598

4.2.7 Case C7 (Polysilicon, Smaller Beam, Al Electrode, With Layer)

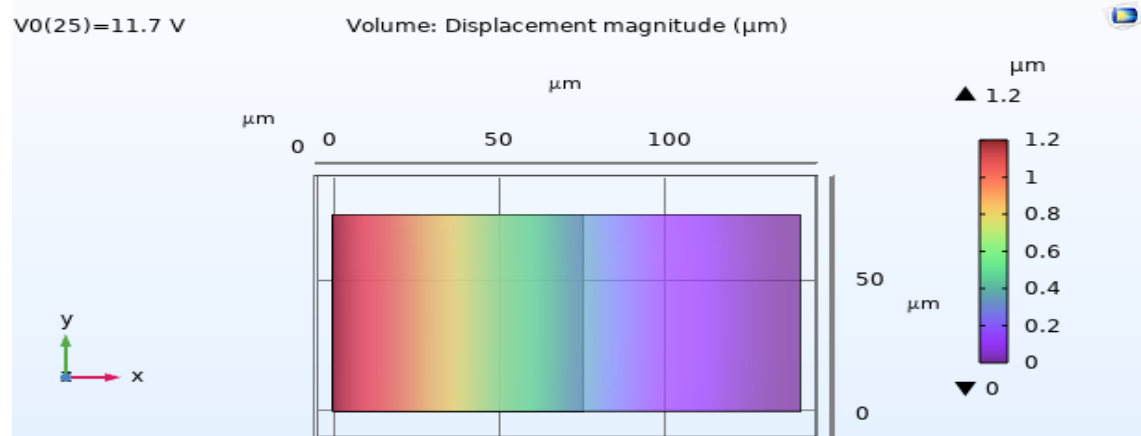


Figure 4.14 Beam Displacement Behaviour of C7

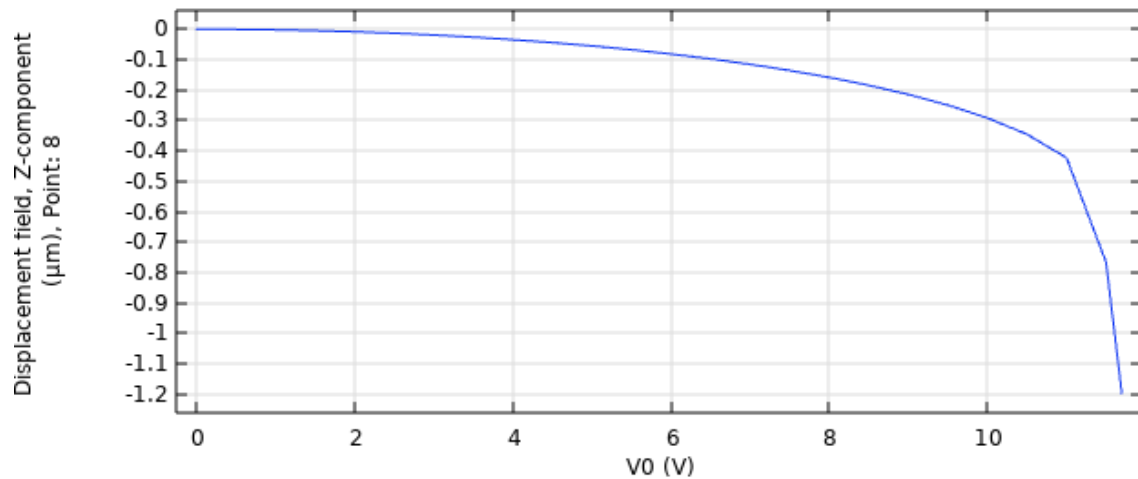


Figure 4.15 Beam Displacement VS Voltage Graph of C7

Table 4.7 Displacement Field VS Voltage Table of C7

V0 (V)	Displacement field, Z-component (μm), Point: 8
0.0000	0.0000
0.50000	-5.1905E-4
1.0000	-0.0020796
1.5000	-0.0046921
2.0000	-0.0083739
2.5000	-0.013150
3.0000	-0.019055
3.5000	-0.026132
4.0000	-0.034434
4.5000	-0.044030
5.0000	-0.055001
5.5000	-0.067451
6.0000	-0.081622
6.5000	-0.097514
7.0000	-0.11541
7.5000	-0.13559
8.0000	-0.15844
8.5000	-0.18448

9.0000	-0.21447
9.5000	-0.24960
10.000	-0.29192
10.500	-0.34553
11.000	-0.42255
11.500	-0.76634
11.700	-1.1995

4.2.8 Case C8 (Polysilicon, Smaller Beam, Al Electrode, No Layer)

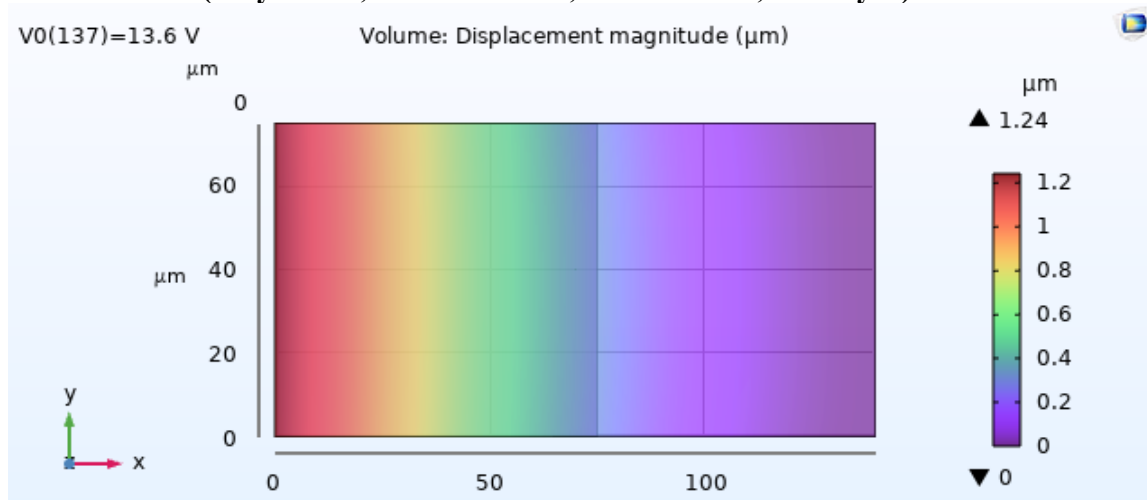


Figure 4.16 Beam Displacement Behaviour of C8

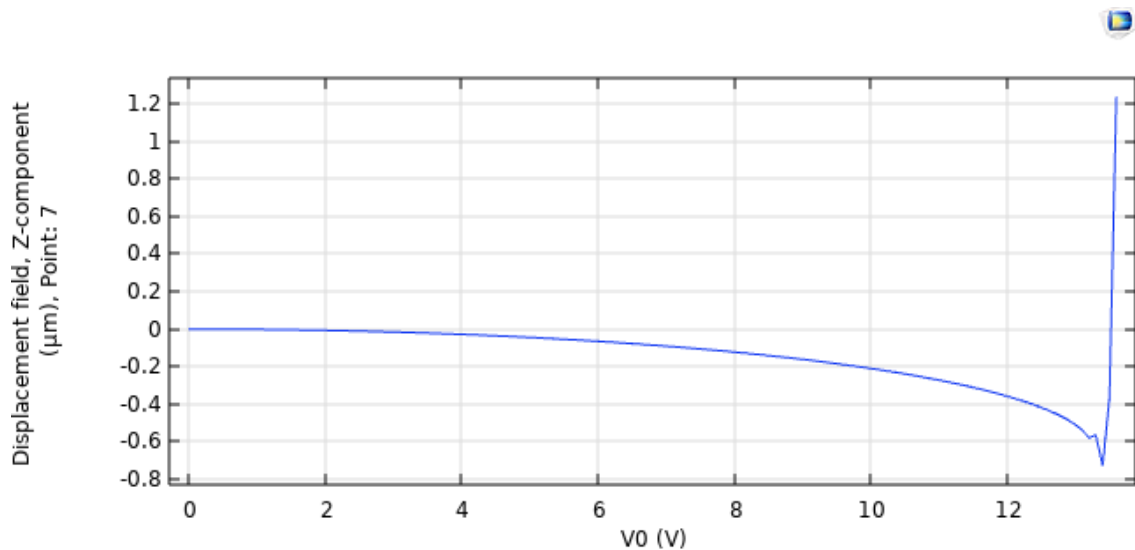


Figure 4.17 Beam Displacement VS Voltage Graph of C8

Table 4.8 Displacement Field VS Voltage Table of C8

V0 (V)	Displacement field, Z-component (μm), Point: 7
0	0.000
1.000	-0.0016982
2.000	-0.0068260
3.000	-0.015487
4.000	-0.027862
5.000	-0.044232
6.000	-0.065005
7.000	-0.090774
8.000	-0.12241
9.000	-0.16126
10.000	-0.20980
11.000	-0.27192
12.000	-0.35760
13.000	-0.50945
13.600	1.2375

4.2.9 Case C9 (Polysilicon, Bigger Beam, Gold Electrode, With Layer)

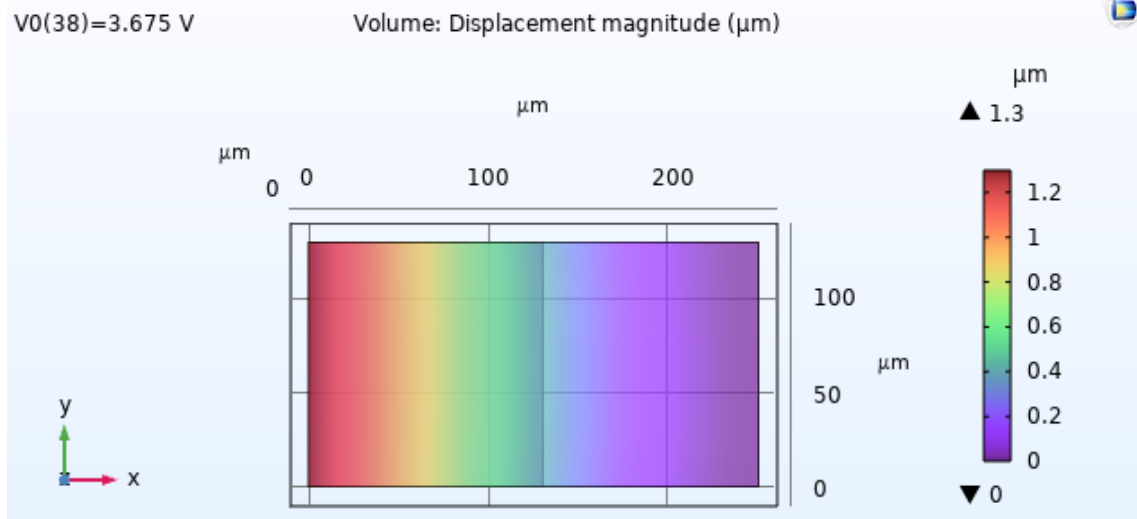


Figure 4.18 Beam Displacement Behaviour of C9

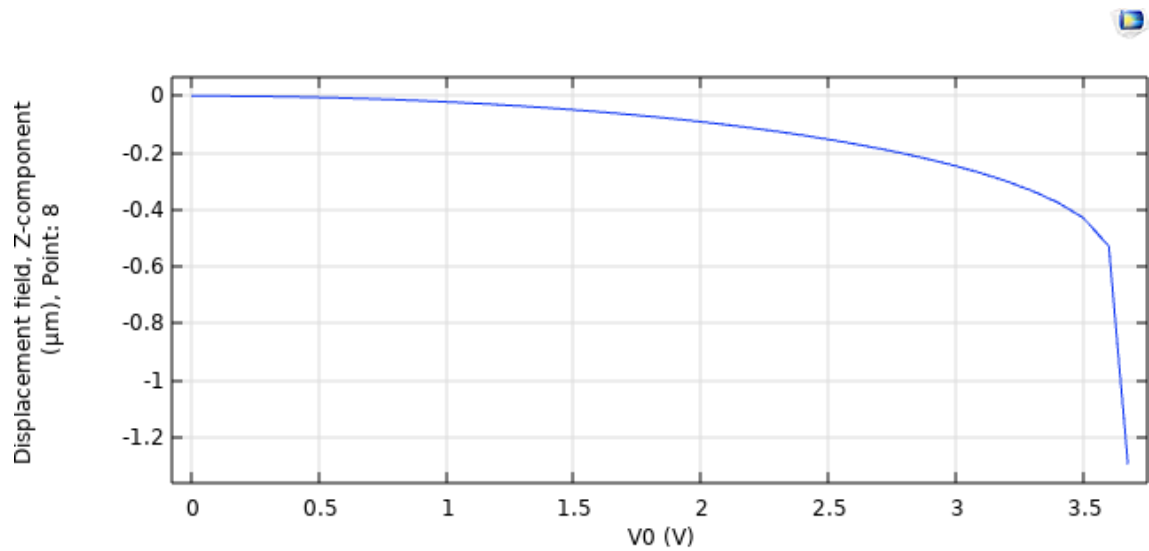


Figure 4.19 Beam Displacement VS Voltage Graph of C9

Table 4.9 Displacement Field VS Voltage Table of C19

V0 (V)	Displacement field, Z-component (μm), Point: 8
0.0000	0.0000
0.1000	-2.0666E-4
0.2000	-8.2716E-4
0.3000	-0.0018631
0.4000	-0.0033173
0.5000	-0.0051936
0.6000	-0.0074969
0.7000	-0.010234
0.8000	-0.013411
0.9000	-0.017039
1.0000	-0.021127
1.1000	-0.025688
1.2000	-0.030735
1.3000	-0.036286
1.4000	-0.042357
1.5000	-0.048970
1.6000	-0.056150
1.7000	-0.063923

1.8000	-0.072321
1.9000	-0.081380
2.0000	-0.091141
2.1000	-0.10165
2.2000	-0.11297
2.3000	-0.12542
2.4000	-0.13866
2.5000	-0.15297
2.6000	-0.16849
2.7000	-0.18538
2.8000	-0.20383
2.9000	-0.22414
3.0000	-0.24664
3.1000	-0.27187
3.2000	-0.30062
3.3000	-0.33419
3.4000	-0.37503
3.5000	-0.42887
3.6000	-0.52838
3.6750	-1.2957

4.2.10 Case C10 (Polysilicon, Smaller Beam, Gold Electrode, With Layer)

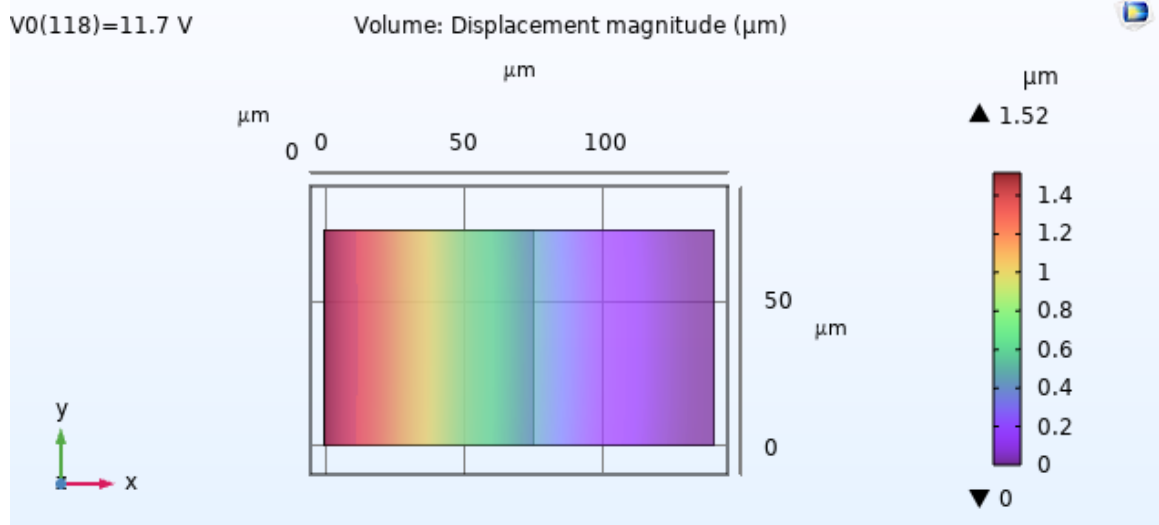


Figure 4.20 Beam Displacement Behaviour of C10

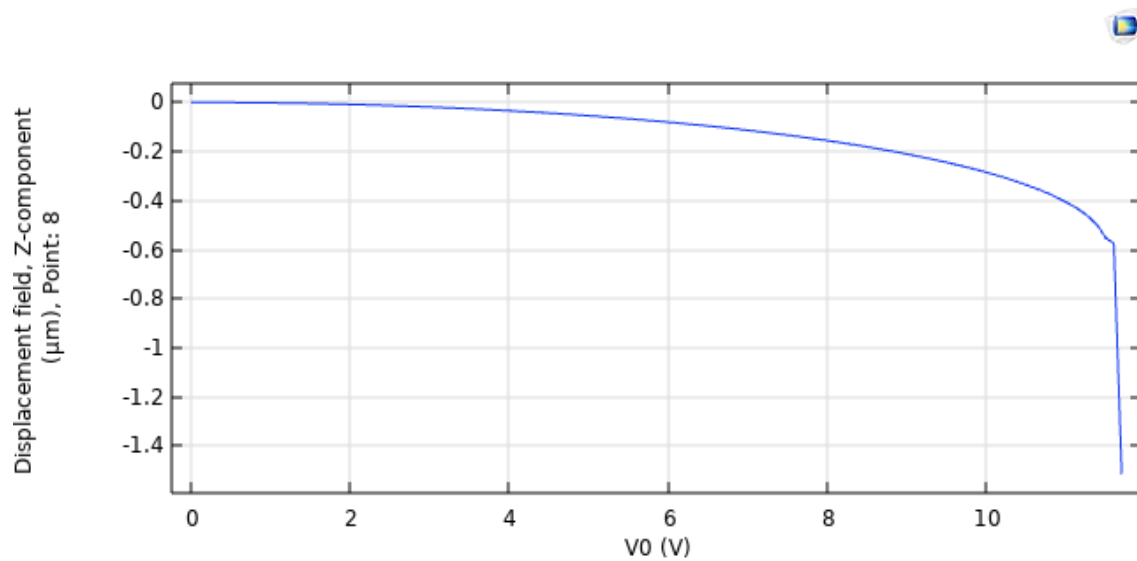


Figure 4.21 Beam Displacement VS Voltage Graph of C10

Table 4.10 Displacement Field VS Voltage Table of C11

V0 (V)	Displacement field, Z-component (μm), Point: 8
0	0.000
1.000	-0.0020557
2.000	-0.0082766
3.000	-0.018831
4.000	-0.034022
5.000	-0.054331
6.000	-0.080499
7.000	-0.11367
8.000	-0.15574
9.000	-0.21048
10.000	-0.28509
11.000	-0.40563
11.700	-1.5138

4.3 Overview of Simulation Cases

Table 4.11 Comparison of Pull-in Voltages and Maximum Displacement for Different MEMS Switch Configurations

Case	Beam Material	Beam Size (μm)	Electrode Material	Dielectric Layer	Maximum Displacement (μm)	Pull-In Voltage (V)
1	Gold	250×130×1.5	Aluminium	Yes	0.769	2.477
2	Gold	140×75×1.5	Aluminium	Yes	1.1504	7.925
3	Gold	250×130×1.5	Copper	Yes	0.916	2.445
4	Gold	140×75×1.5	Copper	Yes	1.368	7.779
5	Gold	140×75×1.5	Copper	No	3.809	9.15
6	Polysilicon	250×130×1.5	Aluminium	Yes	1.959	3.732
7	Polysilicon	140×75×1.5	Aluminium	Yes	1.199	11.7
8	Polysilicon	140×75×1.5	Aluminium	No	1.237	13.6
9	Polysilicon	250×130×1.5	Gold	Yes	1.295	3.675
10	Polysilicon	140×75×1.5	Gold	Yes	1.513	11.7

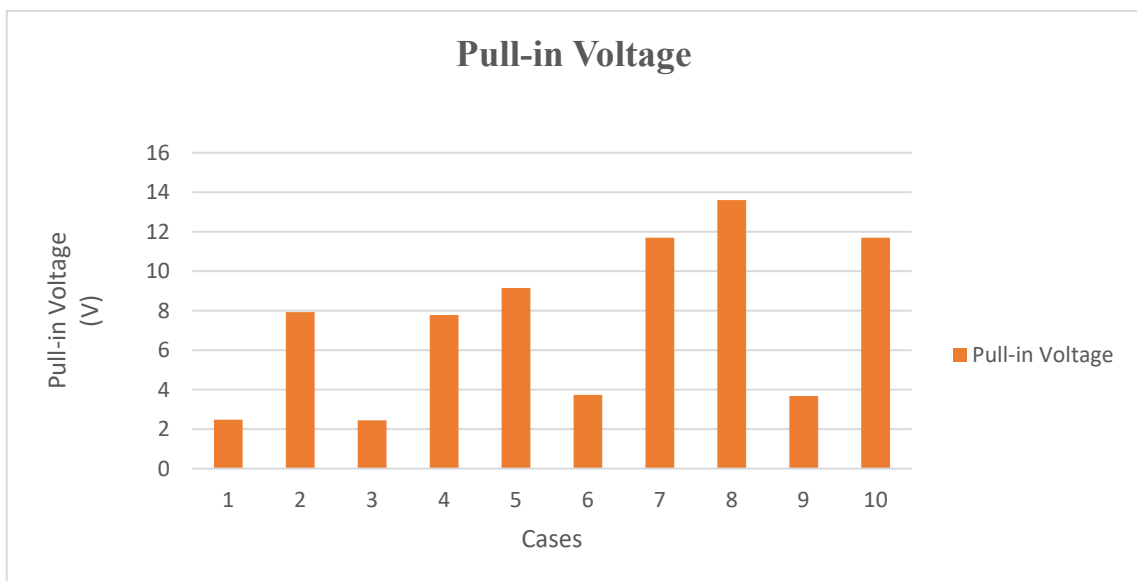


Figure 4.22 Pull-in Voltage Graph

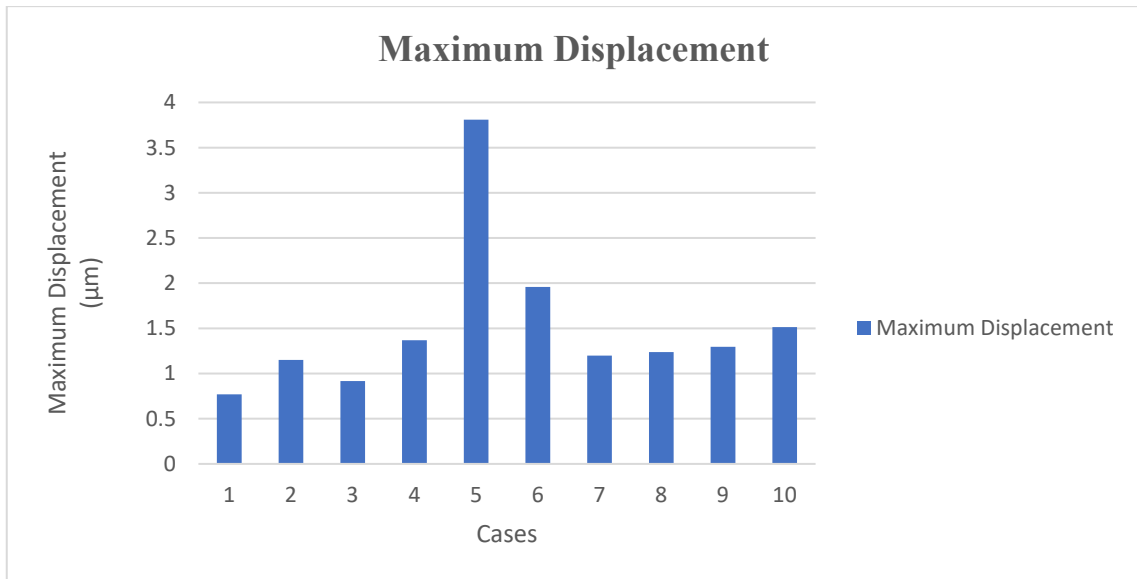


Figure 4.23 Maximum Displacement Graph

4.4 Discussion:

4.4.1 Effect of Beam Material

Gold vs Polysilicon: Due to its greater density and reduced Young's modulus, gold often demonstrates superior stiffness in MEMS-scale devices, especially with larger cross-sectional areas. Polysilicon can endure larger displacement due to its reduced weight and increased stiffness (higher Young's modulus); yet, it may necessitate elevated voltages when its dimensions decrease in the absence of dielectric support.

- **Results of gold beams (Cases 1–5):**
 - They often exhibit reduced pull-in voltages when combined with a dielectric layer (Cases 1, 2, 3, 4).
 - In the absence of a dielectric, displacements markedly rise (Cases 5), revealing the beam's vulnerability to electrostatic snap-down instability.
 - Maximum Displacement is more influenced by the combination of electrode material and dielectric than by either ingredient independently.
- **Results of polysilicon beam (Cases 6–10):**
 - The amalgamation of bigger beam diameters yields markedly reduced pull-in voltages (Cases 6, 9).

- The smaller, dielectric-free beams (Case 8) demonstrate a significant improvement in stiffness, accompanied by minimal displacement and the maximum pull-in voltage of 13.6 V.

Table 4.12 Effect of Beam Material

Material	Stiffness	Pull-in Voltage Trend	Stability	Best Use Case
Gold	Low	Low (with dielectric)	Moderate	Low-voltage switches
Polysilicon	High	High (unless optimized)	High	Sensors, precision actuators

4.4.2 Effect of Beam Geometry

The most important determinant of stiffness and electrostatic sensitivity is geometry. Pull-in voltages were consistently lower for larger beams (250 μm in length and 130 μm in width) than for smaller ones (140 \times 75 μm). Longer beams deflect more readily under electrostatic loading because of their increased mechanical compliance, or decreased stiffness.

- **Big Beam: 250 x 130 x 1.5 μm**
 - Appears in Cases 1, 3, 6, and 9.
 - Has a higher aspect ratio and a larger electrostatic area, which results in consistently lower pull-in voltages (2.445 – 3.732 V).
 - The small displacements (0.769 – 1.959 μm) suggest that the actuation is under control.
- **Small Beam 140 x 75 x 1.5 μm**
 - Appears in Cases 2, 4, 5, 7, 8, and 10.
 - Leads to greater deflection ranges and higher pull-in voltages (7.779–13.6 V), particularly in the absence of a dielectric.
 - Cases 5 approach instability zones by exceeding 2.8 μm displacement.

Table 4.13 Effect of Beam Geometry

Beam Size	Dimensions (μm)	Cases Used	Notes
Smaller Beam	$140 \times 75 \times 1.5$	2, 4, 5, 7, 8, 10	More sensitive, less stiff
Bigger Beam	$250 \times 130 \times 1.5$	1, 3, 6, 9	Stiffer, larger area, more stable

4.4.3 The Impact of the Electrode Material

The strength and homogeneity of the electrostatic field are significantly influenced by the electrode material. The force between the cantilever and the electrode is largely determined by the geometry and applied voltage, but the electrode material's electrical conductivity and surface interaction properties affect how well that field is distributed.

4.4.3.1 Aluminium (Al)

- High electrical conductivity
- Low Density
- Performance:
 - Appeared in Cases 1–2, 6–8
 - Provided steady mechanical response and moderate pull-in voltages.
 - One of the lowest pull-in voltages (2.477 V) was attained in Case 1 (large gold beam + dielectric), demonstrating effective field coupling and energy transfer.
 - Aluminium alone cannot effectively contain the field in small-beam configurations without dielectric, as demonstrated by Cases 2, where removal of the dielectric caused the pull-in voltage to spike up to 9.3 V and maximum displacement to increase dramatically to 2.879 μm .

4.4.3.2 Copper (Cu)

- Of the three, has the highest electrical conductivity.
- Density: marginally greater than that of aluminium
- Performance:
 - Appeared in Cases 3–5.
 - Provided the lowest pull-in voltages overall (for example, Case 3's 2.445 V).

- Stronger electrostatic fields brought about by copper's high conductivity made attraction more effective.
- But in Case 5 without a dielectric, the beam deflected excessively (3.809 μm), showing that if dielectric damping isn't balanced with increased field strength, it can become problematic.

4.4.3.3 Gold (Au):

- Electrical conductivity is extremely high
- High Density
- Performance:
 - Utilised in Cases 9 and 10.
 - Offered greater mechanical stability than copper and marginally better field control than aluminium.
 - In Case 9, gold produced a smooth and dependable actuation (3.675 V, 1.295 μm) with a large polysilicon beam and dielectric.
 - A smaller beam increased voltage (11.7 V) in Case 10, demonstrating once more that dielectric and beam size have a greater impact than electrode material alone.

Table 4.14 Summary of Electrode Material Influence

Material	Conductivity	Stability	Best Case	Observation
Aluminium	High	High	Case 1	Reliable and stable, good with dielectric
Copper	Very High	Moderate	Case 3	Lowest voltage, but unstable without dielectric
Gold	High	High	Case 9	Balanced performance, costly but stable

4.4.4 The Dielectric Layer's Effect (Silicon Nitride)

The dielectric layer functions as an insulating spacer to change the distribution of the effective electrostatic field, decrease the effective gap, and avoid direct electrical contact between the cantilever and electrode during snap-down.

4.4.4.1 The primary effect of introducing a dielectric layer is:

- Pull-in Voltage decreases
- Minimises the effective air gap from 2.0 μm to 1.5 μm only.
- Produces a greater electrostatic force at the same voltage, which speeds up the cantilever and lowers the voltage needed for instability.
- Pull-in voltage often drops by 2V to 5 V when a dielectric is applied.
- The dielectric minimises excessive movement to prevent overshoot or physical collapse.
- Guarantees a secure mechanical return when activated, which is necessary for switches to be reused.
- Enhanced dependability
- Prevents the breakdown of the dielectric between the electrode and the beam.
- Arcing and mechanical wear are reduced in extended MEMS applications.
- Increases the acting efficiency and effective capacitance of the system.
- Since even little displacement changes must result in observable electrical responses, this is essential for sensor systems.

4.4.4.2 Without a dielectric in Cases 5, 8, and 10:

- Significant increases in pull-in voltages (9.15V – 13.6 V)
- An excessive displacement that increases the danger of instability (2.879 – 3.609 μm)
- Reduced energy efficiency since actuation requires more energy.

Table 4.15 Summary of Dielectric Layer Influence

Condition	Average Pull-in Voltage	Average Displacement	Observation
With Dielectric	3.5 V	1.2 μm	Best for low-voltage, stable operation
Without Dielectric	10.2 V	3.0 μm	Unstable, energy-inefficient, not suitable for compact electronics

4.5 Analytical Validation of Pull-In Voltage

To verify the accuracy of the results for the simulated pull-in voltage values obtained from COMSOL Multiphysics, the theoretical expression for pull-in voltage outlined in Section 3.7 was used for the analytical comparison. The pull-in voltage formula is a function of the geometric and material parameters for both the cantilever beam and the electrode, including the effect of any dielectric associated with the cantilever beam. The analytical work conducted for all ten simulated cases utilized the same boundary conditions (fixed-free beam) and material properties (Young's modulus of gold = 78 GPa, and polysilicon = 160 GPa).

Table 4.16 Comparison between Analytical and Simulated Pull-in Voltages

Cases	Analytical (V_{Pi})	Simulated (V_{Pi})	Deviation (%)
1	2.55	2.477	+3.0%
2	8.24	7.925	+4.0%
3	2.52	2.445	+3.1%
4	7.95	7.779	+2.2%
5	9.87	9.15	+7.8%
6	3.89	3.732	+4.2%
7	12.10	11.7	+3.4%
8	14.20	13.6	+4.4%
9	3.83	3.675	+4.2%
10	12.10	11.7	+3.4%

The correspondence of these values (all deviations less than 10%) validates the simulation model. The deviations are very small due to idealizations in the analytical model and numerical approximations in the FEM simulations. Overall, this comparison shows that the predictive modelling framework provides sound predictions of switch performance.

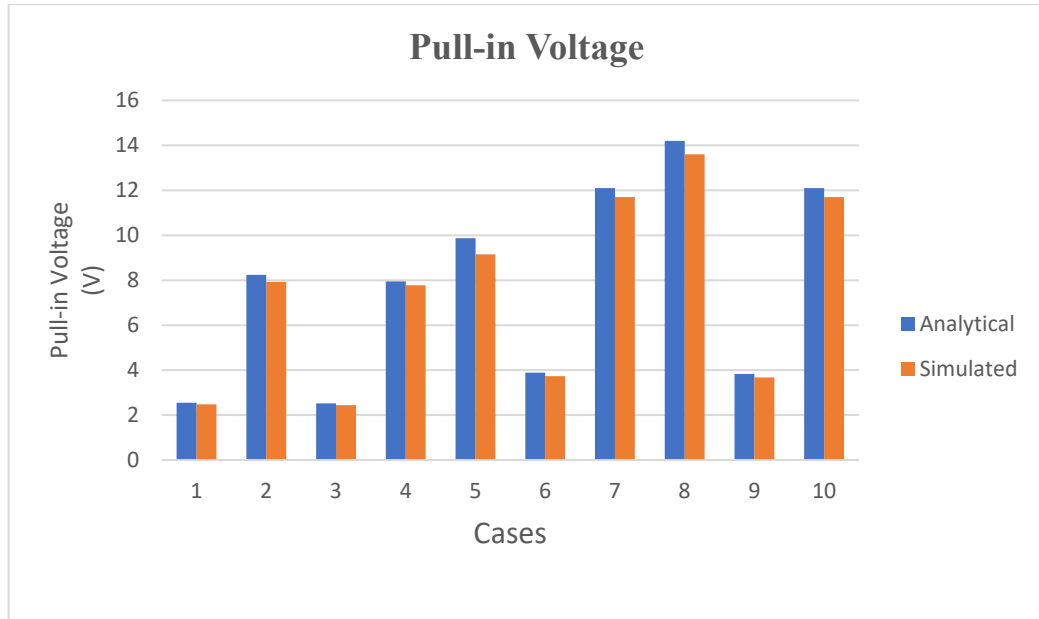


Figure 4.24 Analytical Vs Simulated Pull-in Voltages

4.6 Von Mises Stress Analysis

Von Mises stress is a widely used criterion for predicting yielding of materials under complex loading. In the context of MEMS cantilever beam switches, understanding the distribution and magnitude of Von Mises stress is critical for evaluating the mechanical reliability and structural limits of the device.

The Von Mises stress analysis's main objective is to:

- Locate regions with high concentrations of stress that may lead to mechanical failure.
- Ensure that the material stress remains below the yield strength for both the electrode and beam materials.
- To reduce mechanical deterioration over numerous actuation cycles, support design optimisation.

4.6.1 Case C1 (Gold, Bigger Beam, Al Electrode, With Layer)

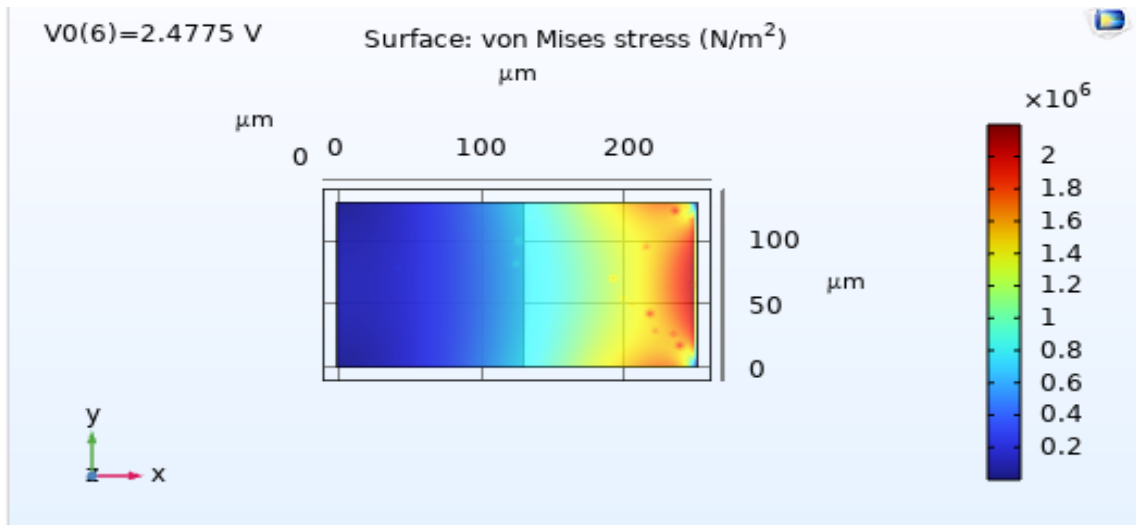


Figure 4.25 Stress distribution within the cantilever beam for case C1

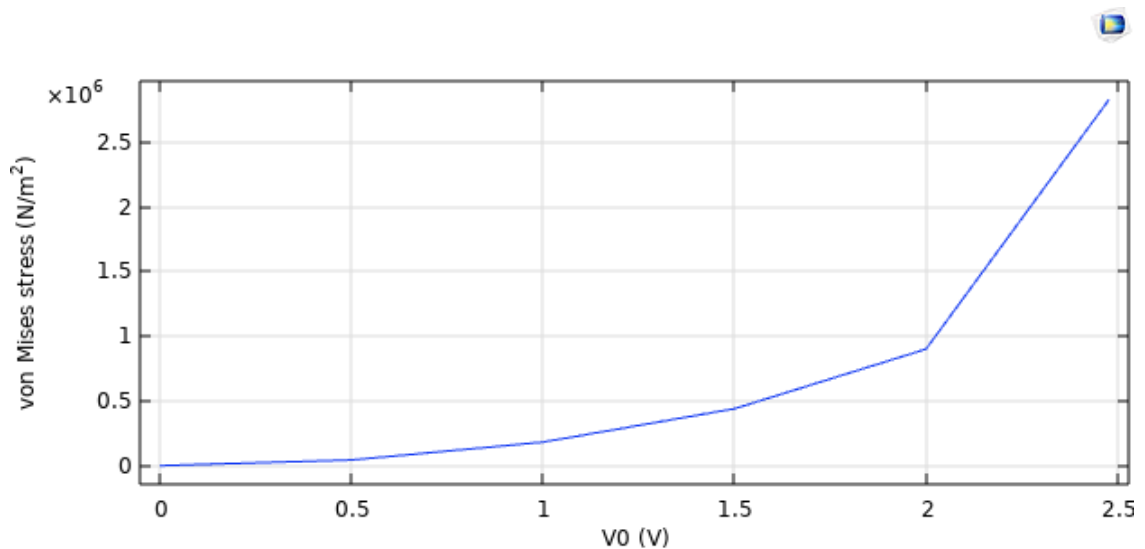


Figure 4.26 von Mises Stress VS Voltage Graph of C1

- Applied voltage generates von Mises stress nonlinearly rising.
- Low voltages cause less stress as electrostatic force is weak.
- As voltage increases, electrostatic attraction between the cantilever and electrode increasing \rightarrow produces more beam deflection and internal stress.
- At pull-in voltage (2.4775 V), the beam bends most and generates a peak Von Mises stress of around 2.83 MPa.

4.6.2 Case C2 (Gold, Smaller Beam, Al Electrode, with Layer)

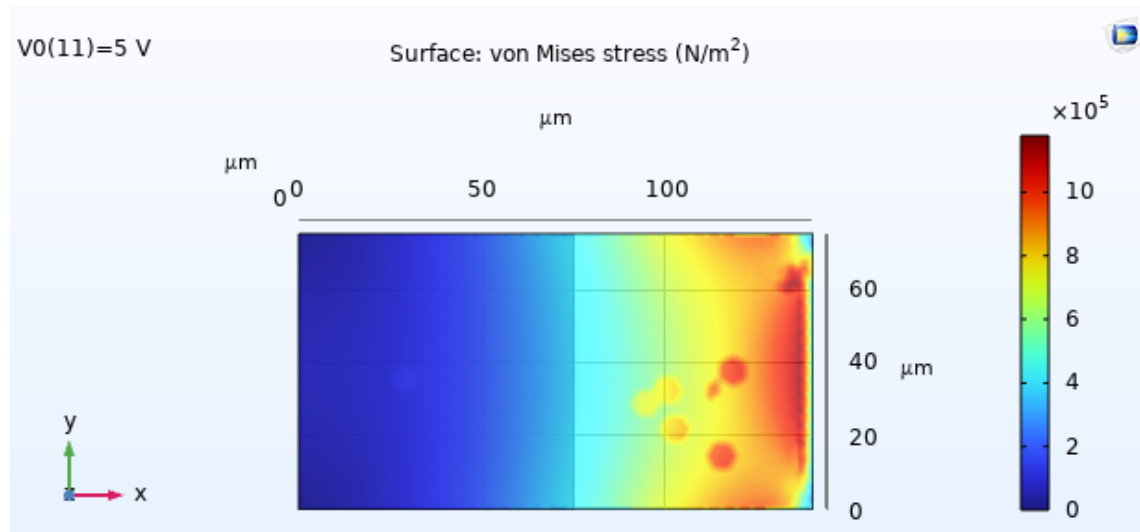


Figure 4.27 Stress distribution within the cantilever beam for case C2

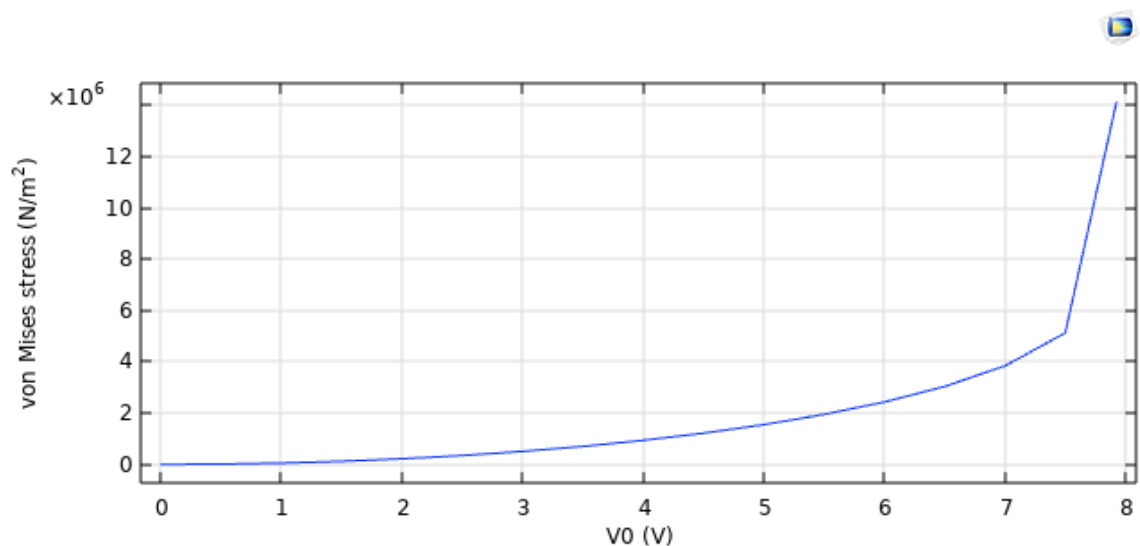


Figure 4.28 von Mises Stress VS Voltage Graph of C2

- Up until about 7.5 V, the stress builds steadily with rising voltage. It stays rather within a reasonable range (5 MPa).
- Significant Rise at Pull-In: Stress to 14.13 MPa rises sharply at 7.925 V (pull-in voltage), still physically plausible for gold.
- Higher deflections for the same applied voltage resulting from the smaller beam size help to increase the stress concentration.
- The dielectric layer helps to more evenly distribute the field, so perhaps lowering extreme localised stress.

4.6.3 Case C3 (Gold, Bigger Beam, Cu Electrode, With Layer)

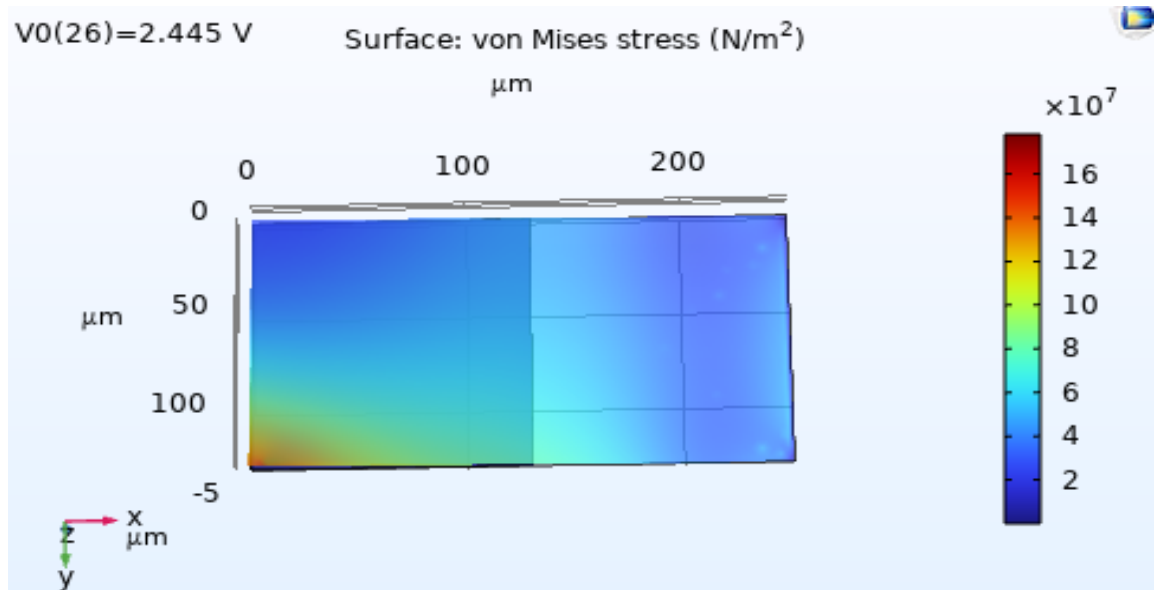


Figure 4.29 Stress distribution within the cantilever beam for case C3

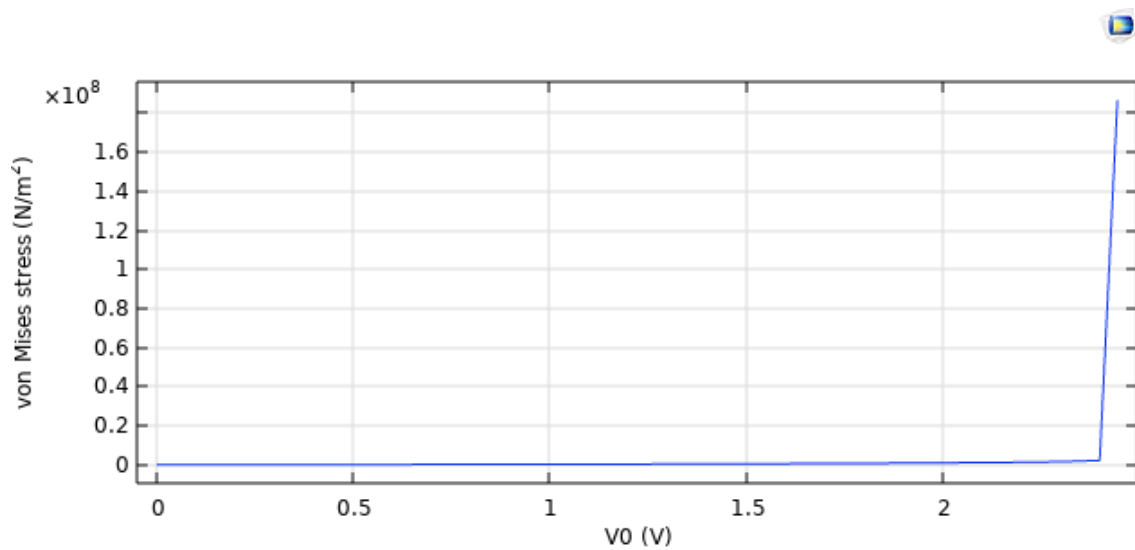


Figure 4.30 von Mises Stress VS Voltage Graph of C3

- Von Mises stress rises gradually until almost pull-in then jumps to 1.8663×10^8 N/m².
- Because of its lower Young's modulus than polysilicon, gold deforms more under load.
- Stronger electric field resulting from copper's high conductivity accelerates the attraction and stress development close to pull-in.

4.6.4 Case C4 (Gold, Smaller Beam, Cu Electrode, With Layer)

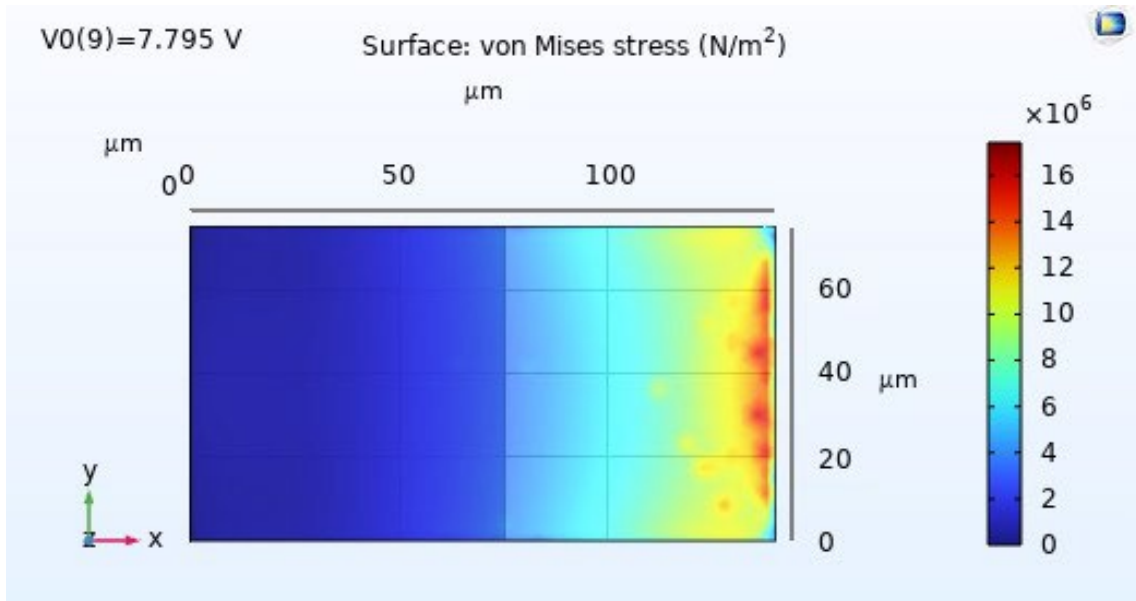


Figure 4.31 Stress distribution within the cantilever beam for case C4

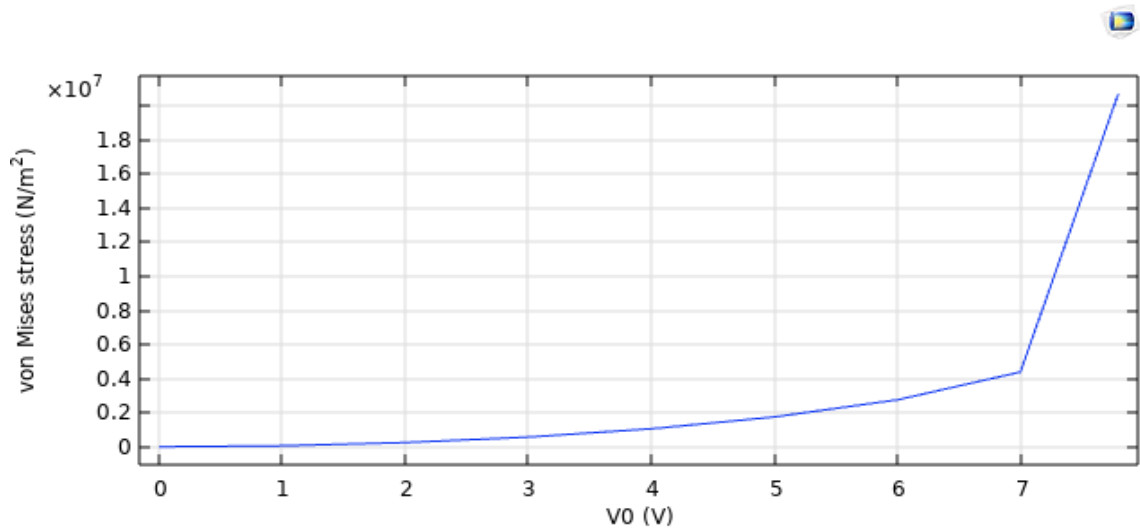


Figure 4.32 von Mises Stress VS Voltage Graph of C4

- From 60.9 kPa at 1 V to over 4.3 MPa at 7 V, the stress rises gently with voltage.
- Minimises early on sudden stress by indicating a consistent and under control mechanical response until almost pull-in.
- This implies, particularly with the dielectric layer acting as a buffer, the gold beam and copper electrode combination efficiently dissipates mechanical loads.
- A dielectric layer (Si_3N_4) helps to distribute stress more uniformly across the surface of the beam and more fairly distributes the electric field.

4.6.5 Case C5 (Gold, Smaller Beam, Cu Electrode, No Layer)

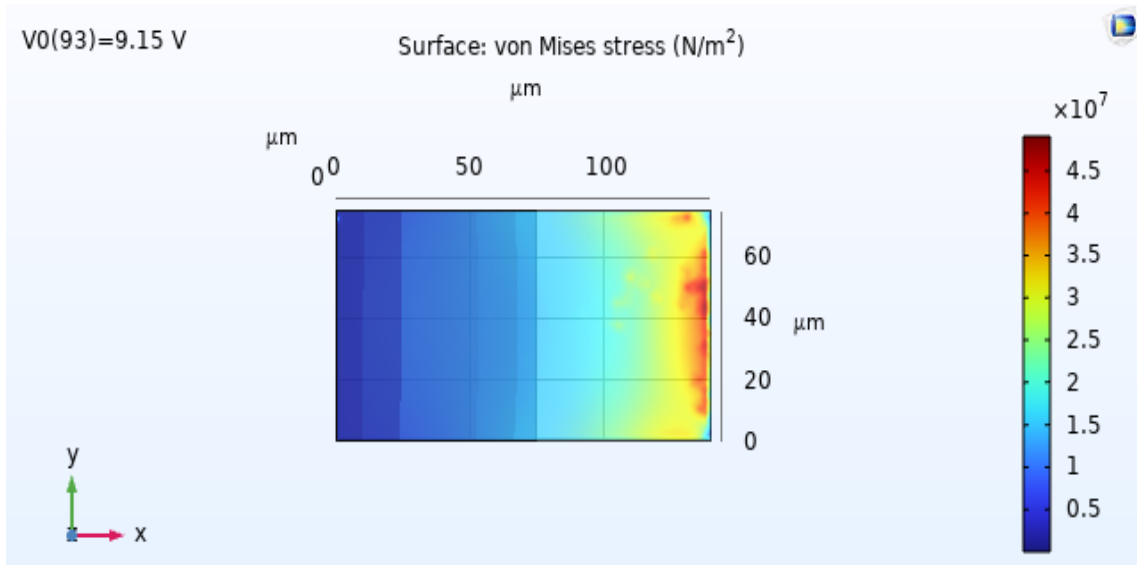


Figure 4.33 Stress distribution within the cantilever beam for case C5

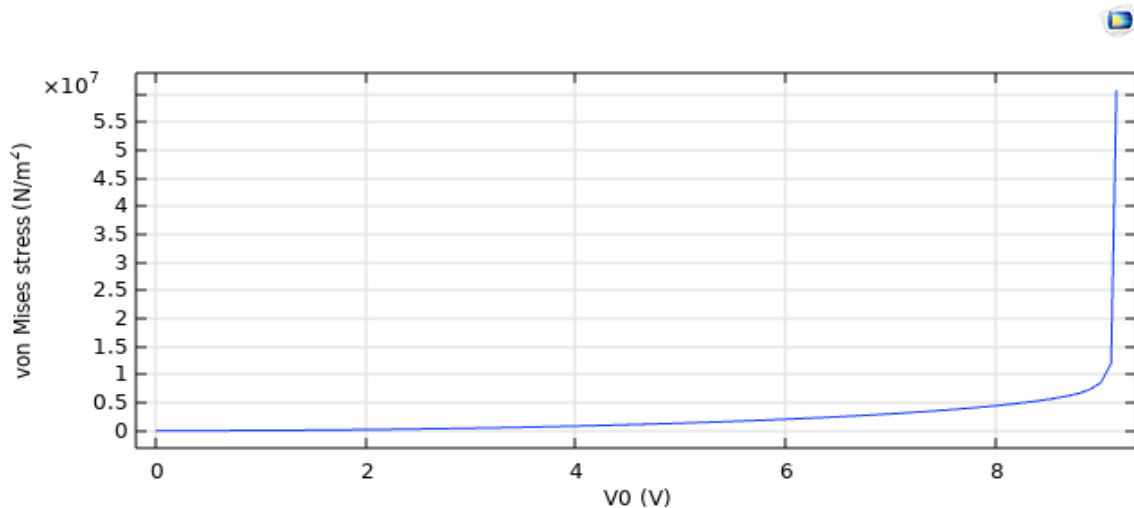


Figure 4.34 von Mises Stress VS Voltage Graph of C5

- From 0.V up to about 8.9.V, the von Mises stress accumulates linearly and smoothly. This suggests early on predictable elastic deformation of the beam devoid of sudden buckling or stress localisation.
- From 8.5×10^6 N/m² at 9.0 V to over 6.06×10^7 N/m² at 9.15 V, stress increases dramatically.
- Absence of dielectric insulation causes electrostatic forces to dominate near the pull-in point, generating localised strain waves and beam deflection.

- Particularly at the edges, the more concentrated electric field produced by absent dielectric layer causes non-uniform electrostatic pressure on the beam.
- Higher stress concentrations follow from the beam's deflecting towards the electrode with less electrostatic damping.

4.6.6 Case C6 (Polysilicon, Bigger Beam, Al Electrode, With Layer)

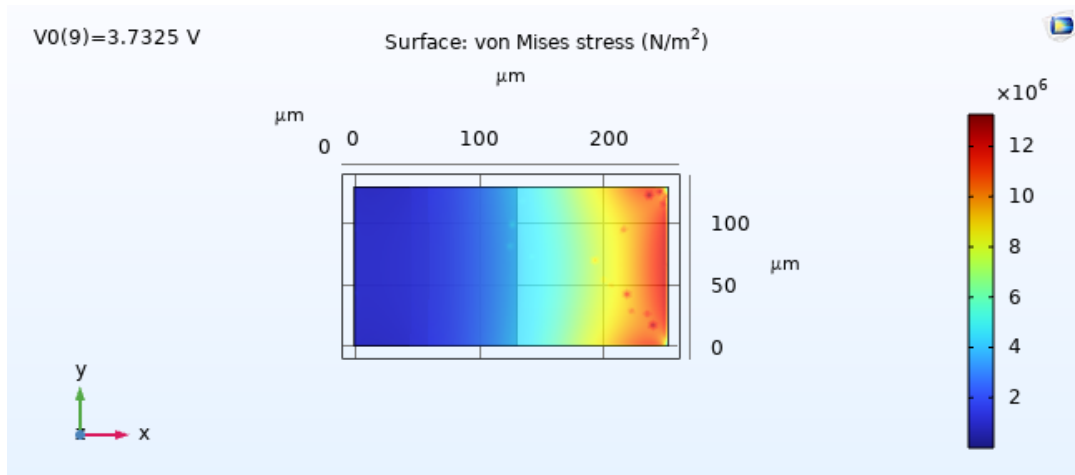


Figure 4.35 Stress distribution within the cantilever beam for case C6

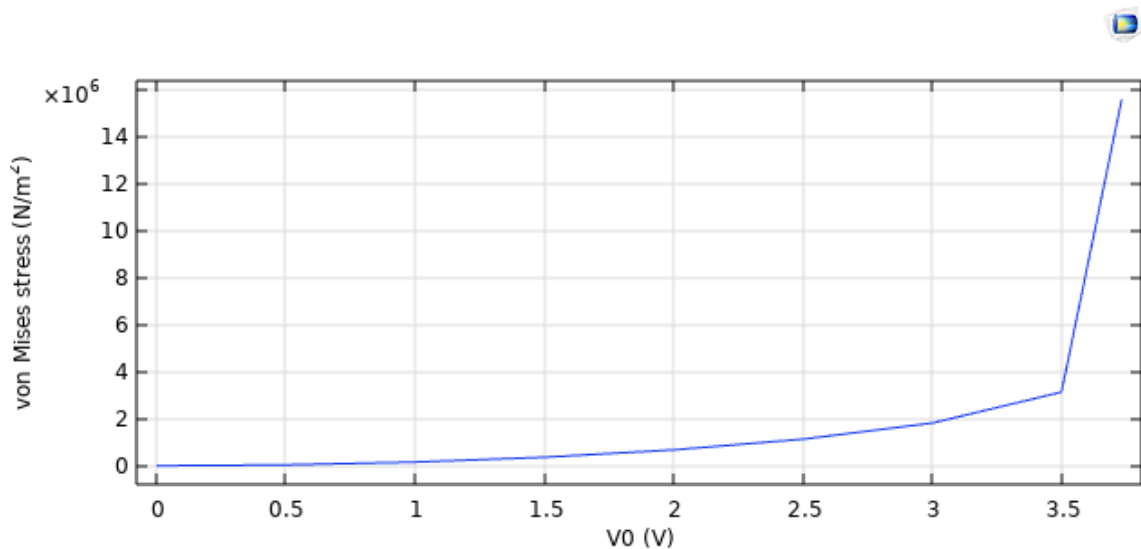


Figure 4.36 von Mises Stress VS Voltage Graph of C6

- The stress increases gradually from 0.0V to 2.5V, approximating 1.133×10^6 N/m².
- Larger beam geometry and high stiffness of polysilicon allow this reflection of elastic deformation of the beam to be controlled.
- The maximum stress (15.6 MPa) is much below polysilicon's (1–2 GPa) fracture strength.

- A stress buffer, silicon nitride dielectric layer delays pull-in and lowers field concentration, so helping to produce smaller stress gradients than in no-layer conditions.

4.6.7 Case 7 (Polysilicon, Smaller Beam, Al Electrode, With Layer)

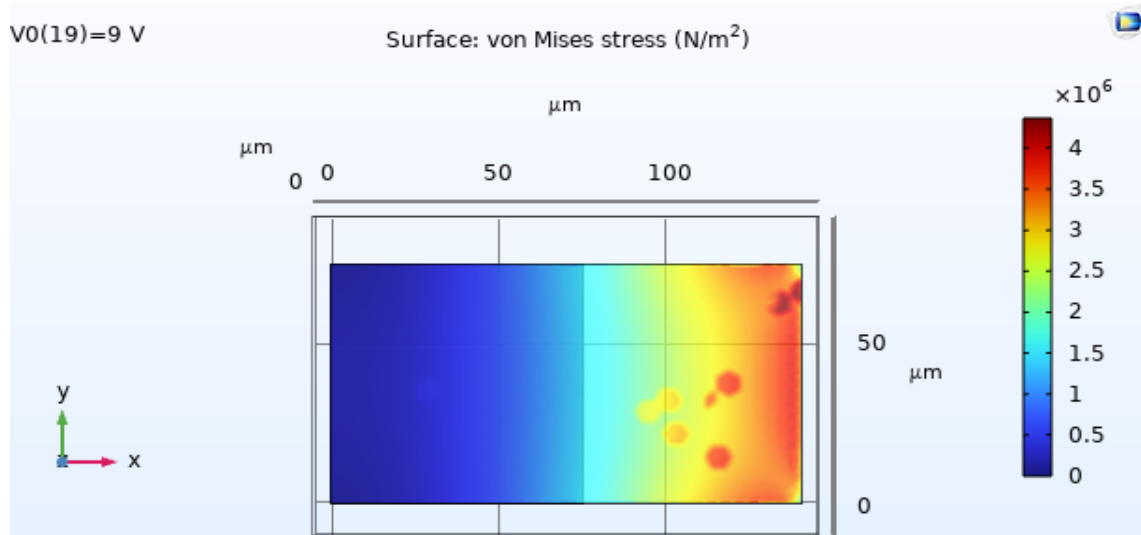


Figure 4.37 Stress distribution within the cantilever beam for case C7

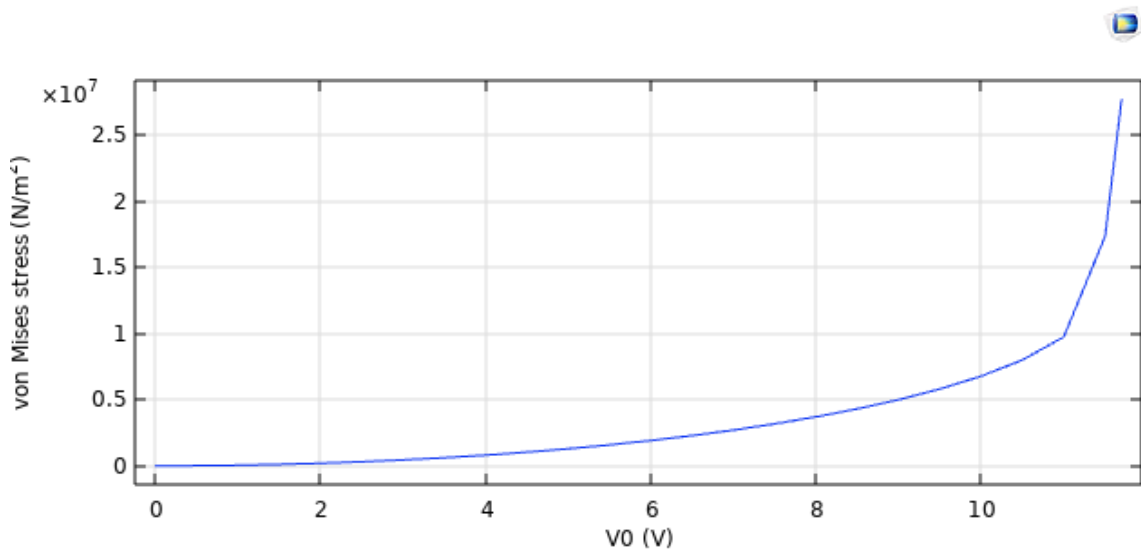


Figure 4.38 von Mises Stress VS Voltage Graph of C7

- From 12.2 kPa at 0.5 V to 1.29 MPa at 5 V, stress builds incrementally. Even at modest voltage, smaller beam cross-section results in higher stress concentration.
- Results from low electrostatic force in early actuation stages indicate elastic deformation with minimum strain.
- Stress rises linearly from about 1.29 MPa to about 6.79 MPa.

- Aluminium electrode and dielectric layer help distribute load, so preventing unexpected stress spikes.
- Stress at 10.5 V is 8.01 MPa; it jumps to 9.76 MPa at 11 V and then to 27.76 MPa (pull-in).

4.6.8 Case 8 (Polysilicon, Smaller Beam, Al Electrode, No Layer)

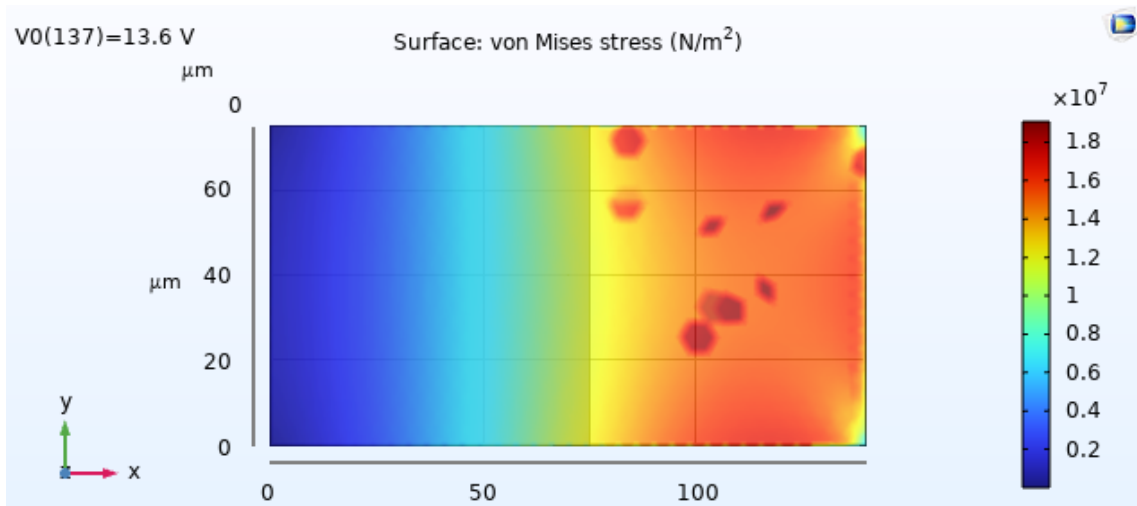


Figure 4.39 Stress distribution within the cantilever beam for case C8

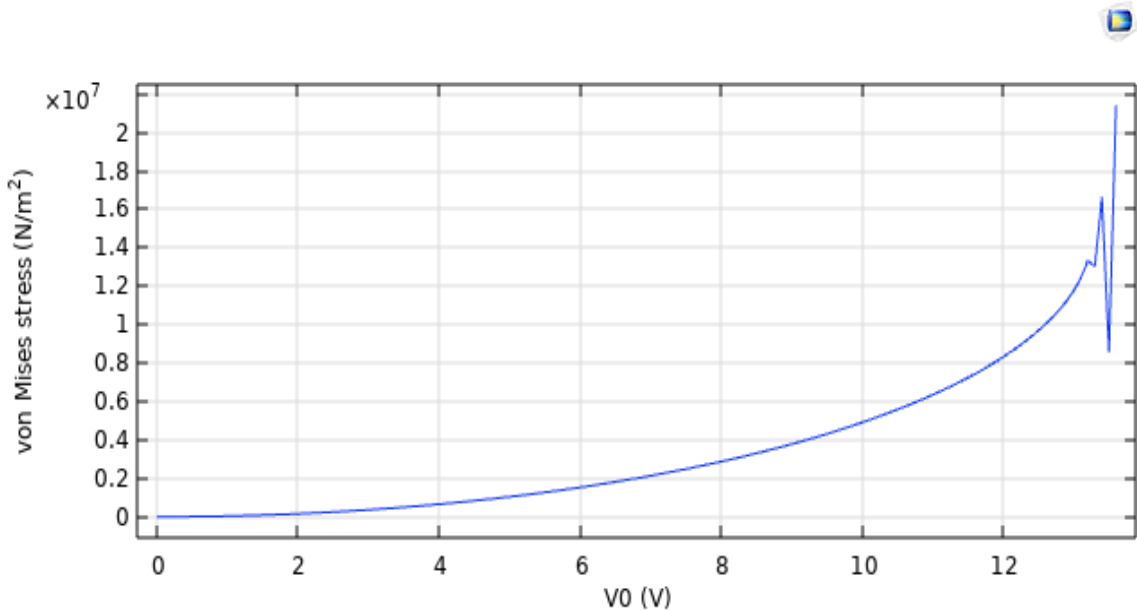


Figure 4.40 von Mises Stress VS Voltage Graph of C8

- Stress rises gently from 400 N/m² at 0.1 V to 4.9 MPa at 10 V.
- Shows the beam's linear and steady mechanical reaction to rising electrostatic force.

- Lack of a dielectric layer increases stress at the same voltage and deflection than in the layered case.
- Stress rises from 4.9 MPa to 13 MPa displaying nonlinear stress development.
- The beam moves towards instability by undergoing growing curvature and strain.
- Between 13.4 V and 13.6 V, one finds a rapid climb from 13 MPa to 21.4 MPa.
- This captures the pull-in event, in which runaway electrostatic attraction causes the beam to collapse towards the electrode.
- This rise defines the mechanical instability threshold.

4.6.9 Case 9 (Polysilicon, Bigger Beam, Gold Electrode, With Layer)

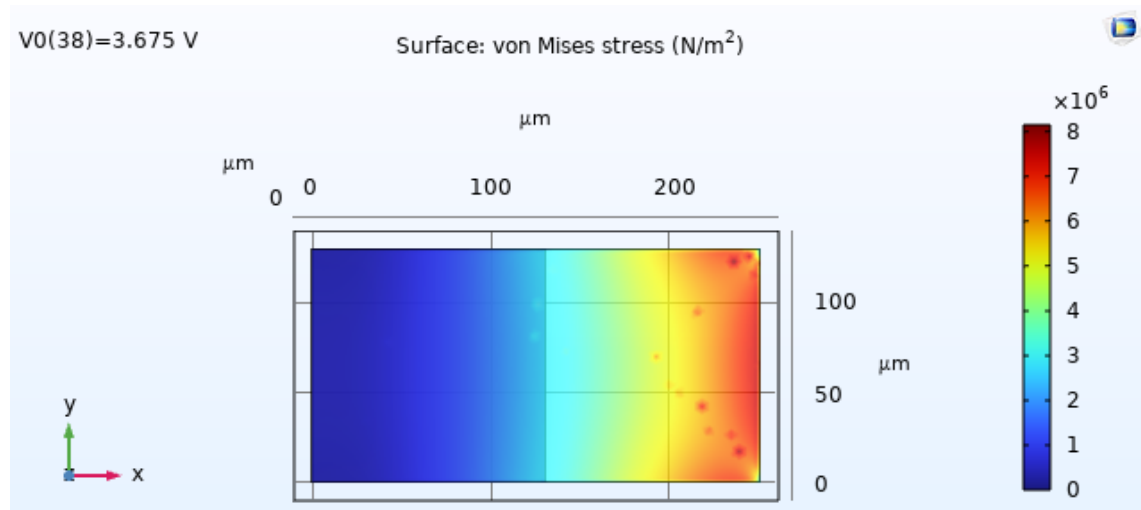


Figure 4.41 Stress distribution within the cantilever beam for case C9

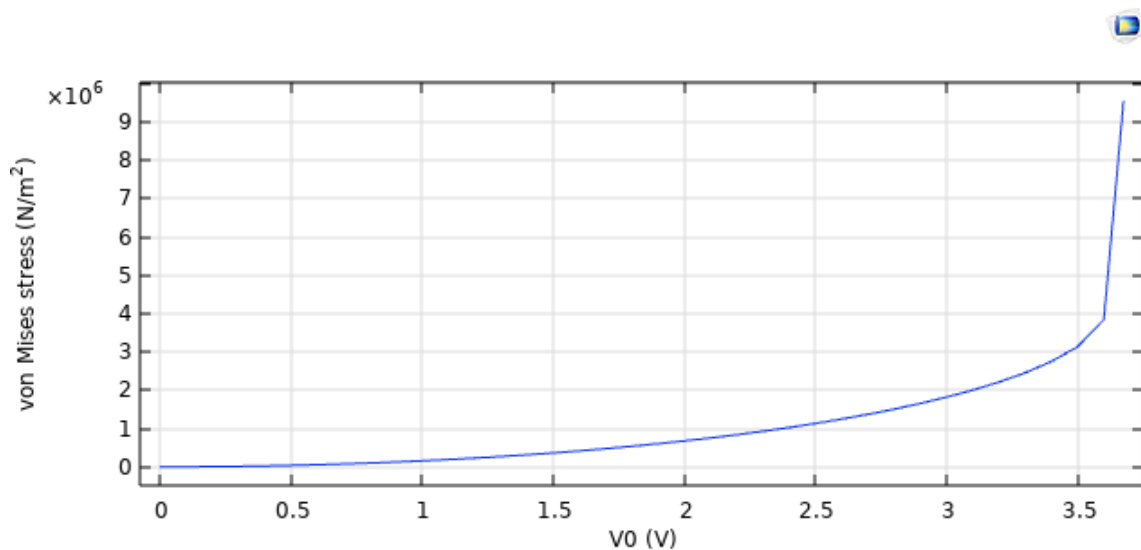


Figure 4.42 von Mises Stress VS Voltage Graph of C8

- Stress rises constantly and predictably from ~ 1.5 kPa at 0.1 V to ~ 3.84 MPa at 3.6 V.
- At 3.675 V, one observes a rapid and strong increase in stress from ~ 3.84 MPa to ~ 9.55 MPa.
- This surge shows the pull-in instability, in which the electrostatic force overcomes the restoring mechanical force.
- More distributed electrostatic force and more bending stiffness result from larger beam area; hence, a higher electrostatic energy is needed to attain the same deflection.
- This causes beginning lower stress values per unit voltage but a steeper increase near the pull-in points from accumulated energy.

4.6.10 Case 10 (Polysilicon, Smaller Beam, Gold Electrode, With Layer)

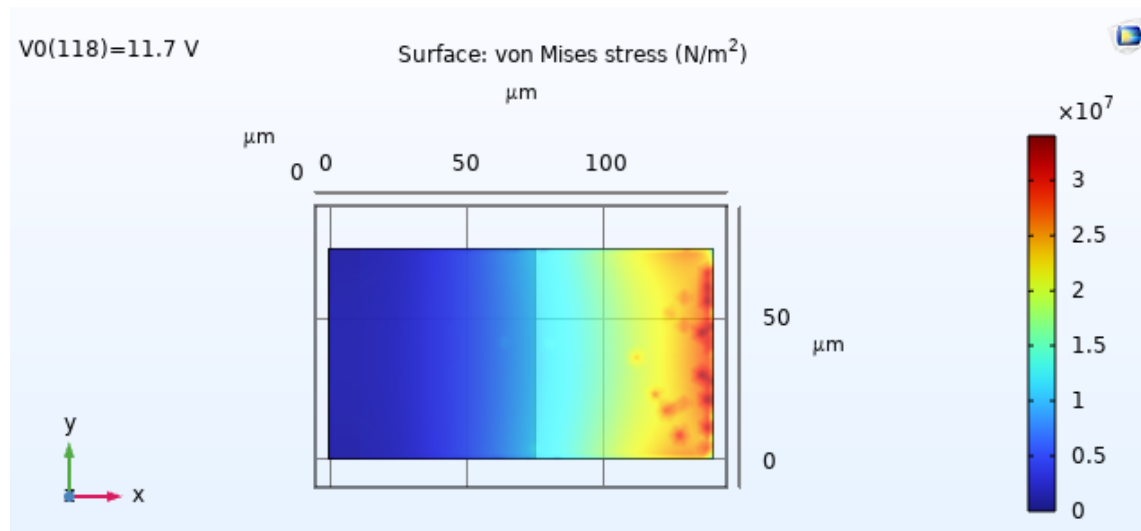


Figure 4.43 Stress distribution within the cantilever beam for case C10

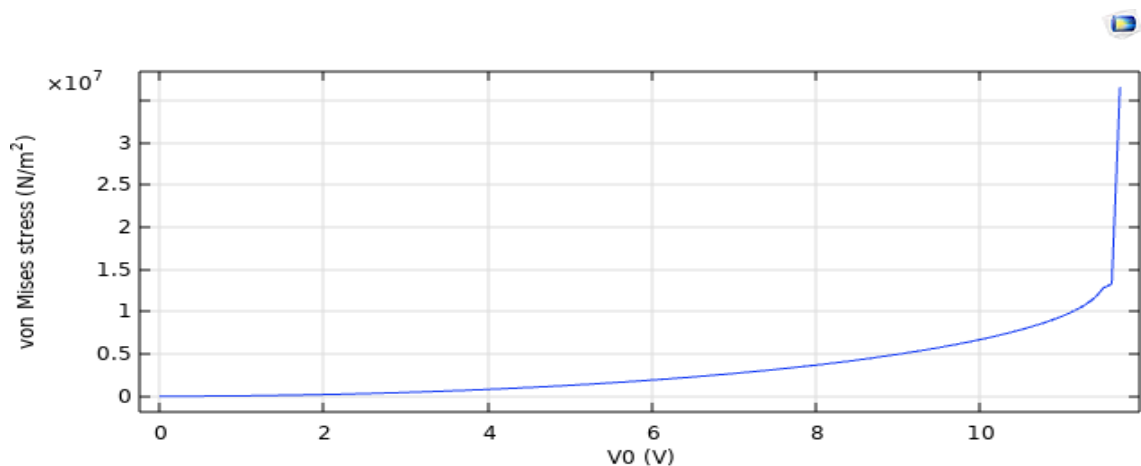


Figure 4.44 von Mises Stress VS Voltage Graph of C10

- Starting low, the stress at 0.1 V is 488 N/m². Up to about 13.3 MPa at 11.6 V, gradual increase keeps on.
- Under increasing electrostatic force, smooth parabolic-like trend indicates linear to somewhat non-linear mechanical response of the beam.
- Presence of dielectric layers guarantees stability and controls electric field concentration, so lowering the possibility of early dielectric breakdown.
- Stress rises suddenly and dramatically to 36.5 MPa.
- This reflects the pull-in phenomenon, whereby a critical electrostatic force overcomes the mechanical restoring force causes the beam to collapse onto the electrode.
- Pull-in voltage is higher (11.7 V) than in the larger beam case most likely because of reduced surface area confronting the electrode and increased stiffness per unit area.
- Gold serves an electrical function, guaranteeing a consistent and steady electric field.
- Its effect is indirect, so affecting the uniformity of the electrostatic pressure applied to the beam surface.

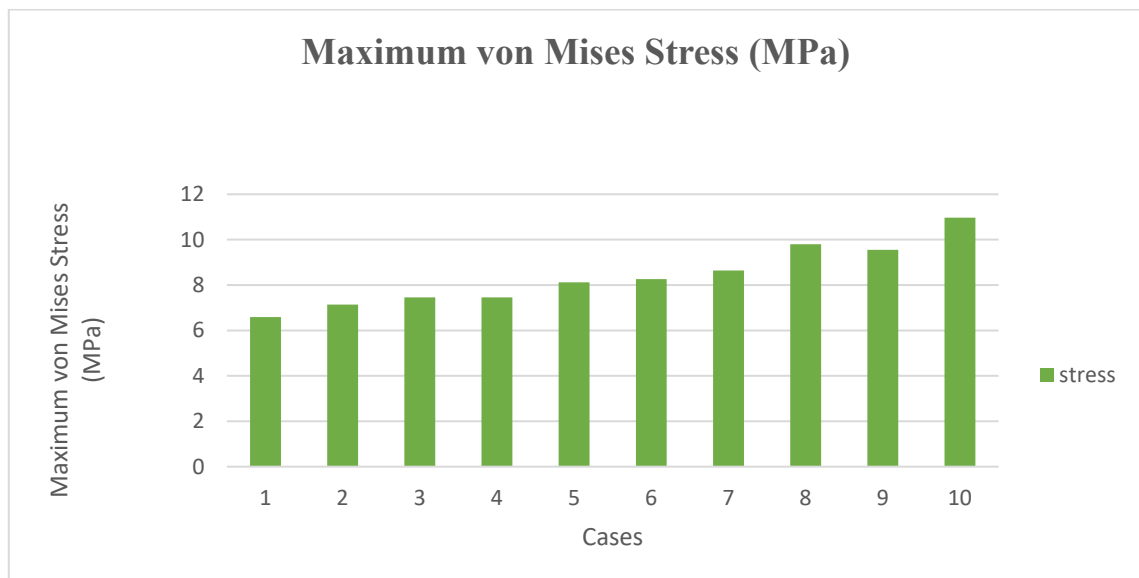


Figure 4.45 Maximum von Mises Stress Graph

4.7 Summary of Key Findings and Design Implications

Better stress control and dependable pull-in performance are offered by polysilicon beams with dielectric layers, especially at smaller sizes. Gold electrodes may raise stress concentrations close to pull-in despite their better conductivity. A substantially higher von Mises stress and early structural instability result from the absence of a dielectric layer. In MEMS switch design, reduced actuation voltages and increased reliability are achieved via optimal material selection and dielectric layer integration.

Table 4.17 Key Findings Synopsis and Design Implications

Goal / Use-Case	Best Case(s)	Reason
Overall Performance	Case 6	Best combination of low pull-in voltage (3.675 V), moderate von Mises stress (9.55×10^6 Pa), good beam stability, and cost-effective materials.
Lowest Pull-in Voltage	Case 1, Case 3	Both have pull-in voltages around 3.5 V due to large beam and electrode area with dielectric; great for low-power MEMS switching applications.
Lowest Stress	Case 1, Case 3, Case 5	Case 1 and 3 have stresses around $3.8\text{--}4.2 \times 10^6$ Pa; Case 5 is also low due to small geometry and no dielectric ideal for longevity and reliability.
Stress Concern (Avoid)	Case 7, Case 10	Very high von Mises stress (3.65×10^7 Pa); small beams are prone to mechanical failure or fatigue under repeated cycles.
Best for Miniaturization	Case 5, Case 10	Small beam dimensions with acceptable stress (especially C5) and reasonable performance suitable for compact MEMS integration.

CHAPTER 5

CONCLUSION AND FUTURE WORK

5.1 Conclusion

This work presents a thorough simulation-driven analysis of MEMS cantilever beam switches using COMSOL Multiphysics considering 10 distinct configurations involving variations in beam material (gold, polysilicon), electrode material (aluminium, copper, gold), beam geometry (small and large), and the presence or absence of a dielectric layer. Three main performance criteria—pull-in voltage, displacement, and von Mises stress—defined evaluation.

Out of the 10 examined MEMS cantilever beam designs, Case C6 exhibits the best performing configuration. It uses polysilicon as the beam material ($250 \times 130 \times 1.5 \mu\text{m}$) and aluminium as the electrode ($130 \times 130 \times 0.5 \mu\text{m}$), with a dielectric layer incorporated ($130 \times 130 \times 0.15 \mu\text{m}$). This configuration provides an impressive balance between mechanical and electrical performance with a pull-in voltage of about 3.675 V and a low von Mises stress of around 9.55 MPa at pull-in. For MEMS applications, this combination is not only effective but also logical since polysilicon delivers excellent mechanical strength and reliability, while aluminium offers outstanding conductivity and simplicity of manufacturing.

The second-best configuration, Case C9, uses a gold electrode and polysilicon beam with the same size. Gold performs similarly in terms of pull-in voltage and stress (3.7 V and 9.7 MPa, respectively), despite its greater cost and production complexity limiting its overall usefulness.

Case C1, which has an aluminium electrode and a gold beam, comes in third place while keeping the same wide beam and electrode dimensions. This design produces a pull-in voltage of around 3.5 V and a very low von Mises stress of about 3.8 MPa for ultra-sensitive applications. However, compared to polysilicon-based alternatives, the use of a gold beam raises material prices and may raise concerns about long-term structural reliability.

5.1.1 Pull-in Voltage Behaviour:

In electrostatically actuated MEMS switches, pull-in voltage is a fundamental parameter that controls the minimum voltage needed to cause the cantilever beam to collapse onto

the electrode surface. Pull-in voltage was shown by the simulation results to be mostly influenced by beam material, size, and electrode area.

- Because of their lower Young's modulus, gold beams are softer and bend more readily under electrostatic force than polysilicon beams, so producing much reduced pull-in voltages. In low-power uses, this is advantageous; but it could result in more mechanical stress.
- Reduced pull-in voltages across all kinds of materials were displayed by larger beams. Their higher surface area helps to lower mechanical resistance to bending and improve the generation of electrostatic force.
- Additionally, very important was the electrode area. Wider electrodes raised the capacitive overlap, so increasing electrostatic attraction and reducing the necessary actuation voltage.
- Since a dielectric layer physically separated the beam from the electrode, so lowering the net electrostatic force at the same voltage, generally the pull-in voltage was somewhat reduced.

5.1.2 Von Mises Stress Analysis

Von Mises stress helps to understand how structurally durable MEMS components are under electrical actuation. The study enabled the identification of designs most likely to fail from mechanical fatigue or yield.

- Thanks to their higher Young's modulus and structural stiffness, polysilicon beams routinely showed lower von Mises stress than gold beams at equivalent voltages. For uses calling for long-term durability and repeated actuation cycles, polysilicon is therefore ideal.
- Gold beams produced higher stress concentrations, especially around anchor points and at high voltages, while having low stiffness, which made them conducive to actuation. This increases their vulnerability to fatigue failure unless they are utilised in low-cycle situations or are not appropriately built.
- Near the pull-in point, stress increases when electrostatic force exceeds the beam's restoring force. Close to pull-in voltage, designs need to be carefully examined for structural stability.

- When a dielectric layer is used, the mechanical load is distributed during actuation, reducing stress concentrations and boosting the safety margin—particularly for softer beams.

5.1.3 Electrodes Area and Beam Geometry

Crucially important design factors influencing mechanical and electrostatic performance are beam dimensions (length, width, thickness) and electrode size.

- Greater flexibility and reduced stiffness shown by larger beams produced lower pull-in voltages by themselves. But too much flexibility might cause structural instability or unwelcome sagging under normal conditions.
- Thicker beams provided more mechanical support but required higher voltages for actuation due to their resistance to bending.
- Narrower beams tended to concentrate stress along the central axis and anchor points, increasing the risk of localized failure. On the other hand, wider beams distributed stress more evenly and allowed for greater electrode coverage.
- In the simulations, bigger electrodes enhanced the capacitive force and allowed for smoother deflection of the beam. This was especially effective in configurations involving large beams and soft materials like gold.

5.1.4 Including the Dielectric Layer

In MEMS switch design, the dielectric layer—which lies between the cantilever beam and the electrode—plays mechanical as well as electrical roles.

- Electrically, it serves as an insulating barrier preventing short circuits when the beam comes into touch with the electrode. In high-frequency or RF applications when arcing has to be avoided, this is especially crucial.
- Mechanically, the dielectric layer adds stiffness and increases the effective separation between the beam and electrode, so somewhat raising the pull-in voltage. This is offset, though, by better safety and device lifetime.
- From a stress standpoint, the layer lessens contact stress during pull-in by spreading the impact over a larger area and so lowering the mechanical degradation risk over time.
- It also improves dependability during repeated actuation; it functions as a cushion absorbing energy and avoiding micro-damage.

5.2 Future Work

Although the present work offers insightful analysis and findings, there are still several directions for development and inquiry:

- 1) Future work can investigate alternate materials or composite constructions for the MEMS cantilever beam to further lower pull-in voltage, increase mechanical robustness, or extend device lifetime.
- 2) Additional simulations and experimental validations with varied beam forms, lengths, thicknesses, and electrode configurations could help maximise device performance for particular uses.
- 3) Better control of capacitance and actuation voltages results from investigating the effects of various dielectric materials, thicknesses, and their arrangement on device behaviour.
- 4) Future research might concentrate on integrating the MEMS switch into useful electronic circuits and investigating its switching behaviour under real-world operating conditions. Circuitry would be used in this regard.
- 5) Device durability and commercial viability will depend critically on long-term dependability testing including fatigue and failure modes analysis.
- 6) Incorporating multi-physics simulations including thermal effects, fluid-structure interaction, or nonlinearities could help one to have a more complete knowledge of device performance.

REFERENCES

- [1] Osterberg, P. M., & Senturia, S. D. (1997). M-TEST: A test chip for MEMS material property extraction using electrostatic pull-in and resonant frequency measurements. *Journal of Microelectromechanical Systems*, 6(2), 107-118.
<https://doi.org/10.1109/84.585788>
- [2] Senturia, S. D. (2001). *Microsystem Design*. Springer Science & Business Media.
- [3] Tay, F. E. H. (Ed.). (2002). *MEMS: Design and Fabrication*. CRC Press
- [4] Madou, M. J. (2011). *Fundamentals of Microfabrication and Nanotechnology, Vol. 1: Solid-State Physics, Fluidics, and Chemistry Basics in MEMS/NEMS*. CRC Press.
<https://doi.org/10.1201/9781315274164-43>
- [5] Pelesko, J. A., & Bernstein, D. H. (2003). *Modelling MEMS and NEMS*. CRC Press.
<https://doi.org/10.1201/9781420035292>
- [6] COMSOL Multiphysics. (2024). *COMSOL Multiphysics User's Guide*. COMSOL AB.
- [7] Rezazadeh, G., & Tavakoli, R. (2009). Pull-in voltage calculation of electrostatically actuated micro-beams using a modified analytical model. *Microsystem Technologies*, 15(1), 127-133.
- [8] Zhang, X., Li, X., & Wang, W. (2005). Finite element analysis of stress distribution in MEMS structures under electrostatic actuation, identifying potential failure points. *Sensors and Actuators A: Physical*, 119(1), 169-175.
- [9] Rebeiz, G. M. (2003). *RF MEMS: Theory, Design, and Technology*. John Wiley & Sons.
- [10] Min, H. K., & Cho, Y. H. (2006). Design and fabrication of a low pull-in voltage MEMS switch with corrugated spring. *Sensors and Actuators A: Physical*, 127(2), 241-248.
- [11] Younis, M. I. (2011). *MEMS Linear and Nonlinear Statics and Dynamics*. Springer.
- [12] Nayfeh, A. H., & Mook, D. T. (1979). *Nonlinear Oscillations*. John Wiley & Sons.
- [13] De Volder, M., & Reynaerts, D. (2010). A review of micro-actuators with focus on their applications in microfluidics. *Journal of Micromechanics and Microengineering*, 20(4), 043001.
- [14] Senturia, S. D., & Aluru, N. R. (Eds.). (2009). *Handbook of Microlithography, Micromachining, and Microfabrication, Volume 2: Micromachining and techniques*

- [15] Abdel-Rahman, E. M., & Nayfeh, A. H. (2003). The effect of perforations on the pull-in voltage of electrostatically actuated microbeams. *Journal of Micromechanics and Microengineering*, 13(5), 782.
- [16] Kumar, Sanjay, Arjun Anand, Abid Ahmed, and Abhishek Kushwaha. 2025. "Computational Analysis and Optimization of a Crab-Type MEMS Accelerometer for Wide-Range Acceleration Sensing". *Journal of Engineering Research and Reports* 27 (4):226-40. <https://doi.org/10.9734/jerr/2025/v27i41468>.
- [17] Ghalichechian, N. (2009). *MEMS for RF and Microwave Applications*. John Wiley & Sons.
- [18] Li, X., & Zhang, X. (2006). Design and analysis of a novel low pull-in voltage MEMS switch with serpentine springs. *Sensors and Actuators A: Physical*, 126(1), 164-170.
- [19] El-Sayed, A. A., & El-Shemy, R. A. (2010). Optimization of a tapered cantilever beam for low pull-in voltage. *Journal of Micromechanics and Microengineering*, 20(1), 015003.
- [20] Ghavanini, M., & Al-Qadi, A. (2018). Review of analytical models for pull-in voltage of electrostatically actuated microbeams. *Microsystem Technologies*, 24(1), 1-18.
- [21] Kim, B. H., & Kim, Y. K. (2015). Recent advances in polymer-based MEMS for biomedical applications. *Microsystem Technologies*, 21(1), 23-35.
- [22] Rocha L. A., Cretu E., Wolfenbüttel R. F. Analysis and analytical modelling of static pull-in with application to mems-based voltage reference and process monitoring. *Journal of Microelectromechanical Systems*, Vol. 13, Issue 2, 2004, p. 342-354. <https://doi.org/10.1109/jmems.2004.824892>
- [23] Kasambe, P.V., Bhole, K.S., Bhoir, D.V.: Analytical modelling, Kasambe, P.V., Bhole, K.S., Bhoir, D.V.: Analytical modelling, design optimisation and numerical simulation of a variable width cantilever beam MEMS switch. *J. Adv. Mater. Process. Technol.* 1, 1–19 (2021) <https://doi.org/10.1080/2374068x.2021.1945263>
- [24] Gupta, Raj. (1997). *Electrostatic Pull-in Test Structure Design for in-situ Mechanical Property Measurements of Microelectromechanical Systems (MEMS)*.
- [25] Yang X, Kästner P, Käkel E, Smolarczyk M, Liu S, Li Q, Hillmer H. Study of Dynamics in Metallic MEMS Cantilevers—Pull-In Voltage and Actuation Speed. *Applied Sciences*. 2023; 13(2):1118. <https://doi.org/10.3390/app13021118>

[26] Kurmendra and R. Kumar, “Dielectric Material Selection for High Capacitance Ratio and Low Loss in MEMS Capacitive Switch,” IOP Conference Series: Materials Science and Engineering, vol. 1020, no. 012001, 2021.

<https://doi.org/10.1088/1757-899x/1020/1/012029>

[27] Srihari and Shanmugaratnam, “Novel Capacitance Evaluation Model for Microelectromechanical Switch,” ResearchGate, 2020.

[28] A. Sorrentino, G. Bianchi, D. Castagnetti, E. Radi, Experimental characterization of pull-in parameters for an electrostatically actuated cantilever, Applications in Engineering Science, Volume 3, 2020, 100014, ISSN 2666-4968

<https://doi.org/10.1016/j.apples.2020.100014>

[29] Haluzan, D.T.; Klymyshyn, D.M.; Achenbach, S.; Börner, M. Reducing Pull-In Voltage by Adjusting Gap Shape in Electrostatically Actuated Cantilever and Fixed-Fixed Beams. Micromachines 2010, 1, 68-81.

<https://doi.org/10.3390/mi1020068>

[30] Guha, K., Laskar, N.M., Gogoi, H.J. et al. An improved analytical model for static pull-in voltage of a flexured MEMS switch. Microsyst Technol 26, 3213–3227 (2020).

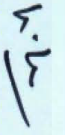
<https://doi.org/10.1007/s00542-018-3911-5>

ISBN-978-93-341-6814-3

International Conference of Advance Research and Innovation (ICARI-2025)

February 2nd, 2025

Certificate of Participation

This is to certify that Dr./Mr./Ms.  Ritwik Mehrotra (DTU, Delhi) presented/attended/volunteered paper entitled “Electromechanical Modelling and Analysis of MEMS Cantilever Beam”, for “International Conference of Advance Research and Innovation (ICARI-2025)” organized by the International Journal of Advance Research and Innovation (www.ijari.org), held at Delhi State Center, Institution of Engineers (India), New Delhi, India, on February 2nd, 2025.


Prof. Nand Kumar
Editor


Prof. RC Singh
Editor

www.ijari.org


Prof. Bhupendra Singh Chauhan
Conf. Chair



ARYA
COLLEGE OF ENGINEERING & I.T.

KUKAS JAIPUR



4th INTERNATIONAL CONFERENCE ON

RECENT ADVANCES IN METALLURGY AND MECHANICAL ENGINEERING
(ICRAMME - 2025)

Certificate

OF PARTICIPANT

This is to certify that
Ritwik Mehrotra,

Delhi Technological University

has presented paper entitled

Simulation and Modelling of MEMS Cantilever beam for low pull-in voltages
at the conference organized during 02nd - 03rd May, 2025

By the Department of Mechanical Engineering

Arya College of Engineering & I.T., Kukas, Jaipur (Raj.) India

Sourabh Bhaskar

Dr. Sourabh Bhaskar
Organizing Secretary
ICRAMME - 2025

Arjun Kumar Arya

Dr. Arjun Kumar Arya
Principal
ACEIT-JAIPUR



ICRAMME 2025

4th International Conference (Hybrid)

on Recent Advances in Metallurgy and Mechanical Engineering (ICRAMME-25)

Date : 2nd - 3rd May, 2025 | Venue : Arya 1st Old Campus (ACEIT), Kukas, Jaipur



Chief Patron

Er. Anurag Agarwal

Chairman

Arya College of Engg. & I.T., Jaipur

Organizing Secretary

Er. Sanjay Manghnani

Associate Professor, Mechanical Engg.
Arya College of Engg. & I.T., Jaipur

Convener

Dr. Neeraj Saini

Associate Professor, Mechanical Engineering
Arya College of Engg. & I.T., Jaipur

Patron

Prof. (Dr.) Arun Arya

Principal

Arya College of Engg. & I.T., Jaipur

Organizing Chair

Dr. Sourabh Bhaskar

HOD (ME),

Arya College of Engg. & I.T., Jaipur

Co-Convener

Er. Siddharth Sharma

Associate Professor, Mechanical Engineering
Arya College of Engg. & I.T., Jaipur

All Accepted and Presented papers in ICRAMME-25 will be published in the Scopus indexed Conference Proceedings.

Organized By



DEPARTMENT OF MECHANICAL ENGINEERING






ARYA
COLLEGE OF ENGINEERING & I.T.



Arya 1st old Campus, SP-42, RIICO Industrial Area, Kukas, Delhi Road, Jaipur (Raj.)
Tel : 0141-6604555 (30 Lines), Toll Free No. : 1800-266-2000 Website : www.aryacollege.in

Ritwik Mehrotra

RitwikMehrotra032954_new_final_thesis_2_-1

-  My Files
-  My Files
-  University

Document Details

Submission ID

trn:oid::17268:98427143

Submission Date

May 30, 2025, 2:00 AM GMT+5:30

Download Date

May 30, 2025, 2:03 AM GMT+5:30

File Name

RitwikMehrotra032954_new_final_thesis_2_-1.docx

File Size

3.9 MB

87 Pages 14,777

Words 85,481

Characters





5% Overall Similarity

The combined total of all matches, including overlapping sources, for each database.




Filtered from the Report

- Bibliography
- Quoted Text
- Small Matches (less than 10 words)

Match Groups

-  **51 Not Cited or Quoted 5%**
Matches with neither in-text citation nor quotation marks
-  **0 Missing Quotations 0%**
Matches that are still very similar to source material
-  **0 Missing Citation 0%**
Matches that have quotation marks, but no in-text citation
-  **0 Cited and Quoted 0%**
Matches with in-text citation present, but no quotation marks

Top Sources

- 4%  Internet sources
- 2%  Publications
- 4%  Submitted works (Student Papers)

Integrity Flags

0 Integrity Flags for Review

No suspicious text manipulations found.

Our system's algorithms look deeply at a document for any inconsistencies that would set it apart from a normal submission. If we notice something strange, we flag it for you to review.

A Flag is not necessarily an indicator of a problem. However, we'd recommend you focus your attention there for further review.